

QCD corrections to charged-current decays with Heavy Sterile Neutrinos in initial or final state and their impact on τ decays

Tim Kretz,^a Ulrich Nierste^a

^a *Institute for Theoretical Particle Physics, Karlsruhe Institute of Technology (KIT), Wolfgang-Gaede-Str. 1, D-76131 Karlsruhe, Germany*

E-mail: tim.kretz@kit.edu, ulrich.nierste@kit.edu

ABSTRACT: Searches for a Heavy Sterile Neutrino N profit from precise predictions of inclusive decay rates, which enter predictions for branching fractions and lifetime. Once the decay channels into semi-hadronic final states are open, a reliable calculation of inclusive decay rates is only possible if N is heavy enough to permit a perturbative calculation, in analogy to the well-known case of semi-hadronic τ lepton decays. We adopt the popular scenario in which N only interacts with the SM particles through N - ν_ℓ mixing, where $\ell = e, \mu, \tau$. Using literature results for W boson correlators calculated to fourth order in the strong coupling α_s , we study the quality of the perturbation series for $N \rightarrow \ell + \text{hadrons}$ to determine the mass ranges for which inclusive decay widths can be predicted in a robust way. We present novel analytic results for the decay rate of $N \rightarrow \tau + \text{hadrons}$ in terms of m_τ/m_N . Our expressions equally apply to $\tau \rightarrow N + \text{hadrons}$, the width of which is found to be perturbatively calculable for $m_N \lesssim 600$ MeV. Applying our result to the τ lifetime, we determine the allowed parameter space for the N - ν_τ mixing angle θ and m_N . We find $|\sin \theta| \leq 0.2$ for $m_N = 600$ MeV and weaker bounds for a lighter N . In the mass region $m_N \geq m_\tau$ we find constraints from the dependence of τ decay rates on $\cos \theta$. Combining $\tau \rightarrow \pi^- \nu_\tau$ and $\tau \rightarrow K^- \nu_\tau$ data gives $|\sin \theta| = (9.09 \pm 3.56) \cdot 10^{-2}$ while N - ν_τ mixing does not improve the agreement between theory and data for $\tau \rightarrow \ell \bar{\nu}_\ell \nu_\tau$. We find current data for the decay rate $\Gamma(\tau \rightarrow \ell + \text{nothing})$ about 1σ above the SM prediction for $\Gamma(\tau \rightarrow \ell \bar{\nu}_\ell \nu_\tau)$, which leads to useful constraints on $\Gamma(\tau \rightarrow \ell X_{\text{dark}})$ or $\Gamma(\tau \rightarrow \ell X_{\text{dark}} X_{\text{dark}})$ with dark-sector particles X_{dark} and might stimulate additional experimental effort on $\tau \rightarrow \ell + \text{nothing}$.

Contents

1	Introduction	1
2	Preliminaries	2
2.1	Sterile neutrino decays at tree level	2
2.2	QCD correlators	3
3	QCD Corrections to Charged Current HSN Decays	7
4	Numerical Analysis	10
4.1	Quality of the perturbation series	10
4.2	Branching ratios of HSN	12
4.3	Constraints on $\theta_{N\tau}$ from the τ lifetime	14
4.4	Contributions on $\theta_{N\tau}$ for $m_N > m_\tau$ from τ branching fractions	18
4.5	Detecting HSN for $m_N < m_\tau$ from spectra	21
4.6	Comparisons	23
4.7	BSM scenarios with other light invisible particles	24
5	Conclusions	24
A	QCD β-Function	26
B	Contour Integration	26
C	Easy-to-use Formulae for Phase-Space Integrals	28
D	Integrated Spectrum	29

1 Introduction

Heavy Sterile Neutrinos (HSNs) (a.k.a. Heavy Neutral Leptons) are a widely-studied extension to the Standard Model (SM), postulated in theories of Dark Matter [1, 2], leptogenesis [3, 4], or neutrino masses [5, 6] (see Ref. [7] for an overview). In standard scenarios it is assumed that HSNs interact with SM particles only through mixing with the active neutrinos ν_e , ν_μ , and ν_τ , so that different observables are highly correlated. In particular, W -mediated weak decays involving an HSN N and a charged lepton ℓ in the initial or final state all involve the same element $V_{N\ell}$ of the matrix describing the mixing of N with the active neutrinos. In the most simple case one assumes that a given HSN N only mixes with one active neutrino ν_ℓ , so that $V_{N\ell}$ reduces to $V_{N\ell} = \sin \theta$ with a neutrino mixing angle θ . It is therefore desirable to study as many different decays as possible to first discover HSNs and subsequently corroborate or falsify the active-sterile mixing concept. In the former case one will aim at the precise determination of $V_{N\ell}$ for $\ell = e, \mu, \tau$. In the latter case one will find apparent different values for $V_{N\ell}$ in different decays and turn the attention to less minimal models featuring new interactions between N and SM fermions, possibly mediated by new Higgs bosons or leptoquarks [8, 9].

The search for HSNs produced at colliders and the interpretation of experimental limits requires accurate predictions of branching fractions. In addition, it is important to know the N lifetime to understand whether N decays outside or within the detector. Especially interesting is the parameter space for which N decays with a displaced decay vertex, which corresponds to an ideal, background-free signal. To predict branching fractions or lifetimes one must calculate the total decay width $\Gamma_{\text{tot}}(N)$. In this paper we consider semi-hadronic decays of N and present precise predictions for $\Gamma(N \rightarrow \ell + \text{hadrons})$ for the case that the HSN mass m_N is large enough that accurate perturbative QCD predictions are possible. To this end we exploit literature results on the correlator of two charged quark currents to five-loop order of QCD [10] and add the appropriate phase-space integration to predict $\Gamma(N \rightarrow \ell + \text{hadrons})$. The main purpose of this analysis is the determination of the range for m_N for which the perturbative calculation is applicable, by requiring that with higher orders in α_s the size of the perturbative correction and the dependence on the unphysical renormalization scale μ decrease. Specifically, if the invariant mass of the hadronic system governed by $m_N - m_\ell$ is too small, perturbation theory breaks down, and the same is true for certain larger values of m_N which are closely above the masses of the D or B mesons. For $\ell = e$ or μ we can simply use the formulae for $\tau \rightarrow \nu_\tau + \text{hadrons}$ decays from the literature [10, 11], but for $\Gamma(N \rightarrow \tau + \text{hadrons})$ we perform a new calculation to account for $m_\tau \neq 0$ and find closed results in terms of m_τ/m_N with polylogarithms (up to α_s^3) or a series representation (at order α_s^4). With this result we can further predict $\Gamma(\tau \rightarrow N + \text{hadrons})$ for the case that m_N is too large to be neglected and analyse the impact of N - ν_τ mixing on τ lifetime and

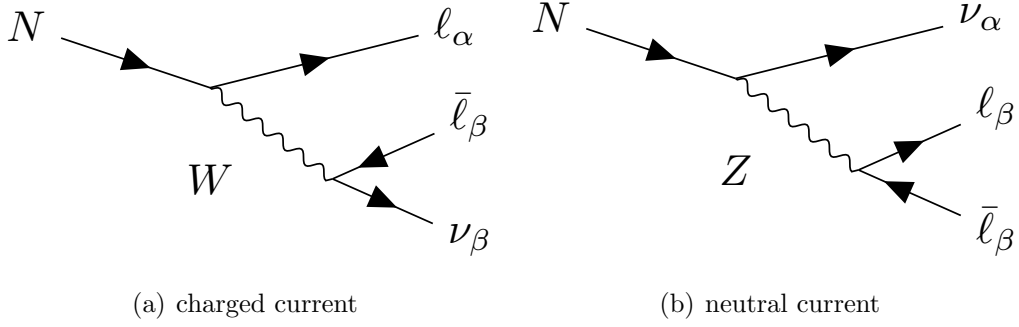


Figure 1. Tree diagrams for an HSN decay. For $\alpha = \beta$ both diagrams interfere. Diagrams were drawn with the help of TikZ-Feynman [18].

branching fractions.

Our paper is organised as follows: In Sec. 2 we recapitulate the known results entering the calculation of the inclusive hadronic HSN decay width, in Sec. 3 we show the details of the actual calculation followed by a discussion of the phenomenology of our results in Sec. 4. We conclude in Sec. 5.

2 Preliminaries

2.1 Sterile neutrino decays at tree level

Several decays of HSN or of leptons and hadrons into HSN have been calculated at tree level [12–17]. Here we briefly collect the tree-level results relevant to our study and introduce our notation.

An HSN N can decay via a W boson into a charged lepton and a quark-antiquark pair (u', \bar{d}'). Here, we only consider cases in which N is heavy enough to permit $N \rightarrow \ell u \bar{d}$ and $N \rightarrow \ell u \bar{s}$ decays, but for large enough values of m_N also final states with $u' = c$ or $d' = b$ can be accessible. The decay width reads

$$\Gamma(N \rightarrow \ell^- u' \bar{d}') = N_c \frac{G_F^2 m_N^5 |V_{N\ell}|^2 |V_{u'd'}|^2}{192\pi^3} \times 12 \int_{(x_{u'}+x_{d'})^2}^{(1-x_\ell)^2} \frac{dx}{x} (1+x_\ell^2-x)(x-x_{u'}^2-x_{d'}^2) \sqrt{\lambda(1, x, x_\ell^2) \lambda(x, x_{u'}^2, x_{d'}^2)}, \quad (2.1)$$

here G_F is the Fermi constant, m_N is the mass of the sterile neutrino, $V_{N\ell}$ parametrises the mixing between N and ν_ℓ , $V_{u'd'}$ is the relevant CKM matrix element, $N_c = 3$ is the number of colours, $x_i = m_i/m_N$, and $\lambda(a, b, c) = (a - b - c)^2 - 4bc$ is the Källén function.

Decay rates of an HSN into leptons $N \rightarrow \ell_i \bar{\ell}_j \nu_j$ are found from Eq. (2.1) by setting $N_c = 1$ and $V_{u'd'} = 1$:

$$\begin{aligned} \Gamma(N \rightarrow \ell_\alpha \bar{\ell}_\beta \nu_\beta) \\ = \frac{G_F^2 m_N^5 |V_{N\ell}|^2}{192\pi^3} \times 12 \int_{x_\beta^2}^{(1-x_\alpha)^2} \frac{dx}{x} (1+x_\alpha^2-x)(x-x_\beta^2) \sqrt{\lambda(1, x, x_\alpha^2) \lambda(x, x_\beta^2, 0)}, \end{aligned} \quad (2.2)$$

where $x_\alpha = m_{\ell_\alpha}/m_N$. This relation only holds for $\alpha \neq \beta$. We dub the lepton directly attached to the HSN the tagging lepton (see Fig. 1). For $\alpha = \beta$ there are additional contributions to the leptonic width due to interference with the neutral current decay. The decay width becomes

$$\begin{aligned} \Gamma(N \rightarrow \nu_\alpha \ell_\alpha \bar{\ell}_\alpha) \\ = \frac{G_F^2 m_N^5 |V_{N\ell}|^2}{192\pi^3} \times \left[\sqrt{1-4x_\ell^2} \left(\left(\frac{g_V^2}{2} + g_V \right) (1-10x_\ell^2 + 18x_\ell^4 - 36x_\ell^6) \right. \right. \\ \left. \left. + \left(\frac{g_A^2}{2} + g_A \right) (1-18x_\ell^2 - 22x_\ell^4 + 12x_\ell^6) + 1 - 14x_\ell^2 - 2x_\ell^4 - 12x_\ell^6 \right) \right. \\ \left. - 24 \left(\left(g_V^2 + 2g_V \right) x_\ell^6 (2-3x_\ell^2) \right. \right. \\ \left. \left. + \left(g_A^2 + 2g_A \right) x_\ell^4 (2-2x_\ell^2 + x_\ell^4) + x_\ell^4 (2-2x_\ell^4) \right) \ln \left(\frac{2x_\ell}{1 + \sqrt{1-4x_\ell^2}} \right) \right], \end{aligned}$$

here $g_A = -1/2$, $g_V = -1/2 + 2s_w^2$ with $s_w = \sin \theta_w$ and the Weinberg angle θ_w . Our results agree with those of Bodarenko et al. in Ref. [7]. In Fig. 2 we show the decay widths as a function of m_N . The widths for e or μ as tagging leptons are almost indistinguishable.

2.2 QCD correlators

The QCD dynamics of decays of HSNs into hadrons is governed by the decays of virtual electroweak gauge bosons into hadrons. The decays of W and Z bosons into hadrons have been calculated up to $\mathcal{O}(\alpha_s^4)$ [10, 19]. Here we use these results to calculate the charged-current contribution to the decay of an HSN.

The optical theorem relates any inclusive decay width to the imaginary part of the self-energy of the decaying particle. The non-trivial part of the W or Z boson self-energy is the correlator of two charged quark currents, namely the time ordered product of the vector and axial vector currents of the quarks $j_{\mu,ij}^{V/A} = \bar{q}_i \gamma_\mu (\gamma_5) q_j$. It may be parametrized as follows [20, 21]

$$\Pi_{\mu\nu,ij}^{V/A}(q, m_i, m_j, \mu, \alpha_s) = i \int dx e^{iqx} \langle 0 | \hat{T} \{ j_{\mu,ij}^{V/A}(x) j_{\nu,ij}^{V/A\dagger}(0) \} | 0 \rangle \quad (2.3)$$

$$= g_{\mu\nu} \Pi_{ij,V/A}^{[1]}(q^2) + q_\mu q_\nu \Pi_{ij,V/A}^{[2]}(q^2) \quad (2.4)$$

$$= (-g_{\mu\nu} q^2 + q_\mu q_\nu) \Pi_{ij,V/A}^{(1)}(q^2) + q_\mu q_\nu \Pi_{ij,V/A}^{(0)}(q^2). \quad (2.5)$$

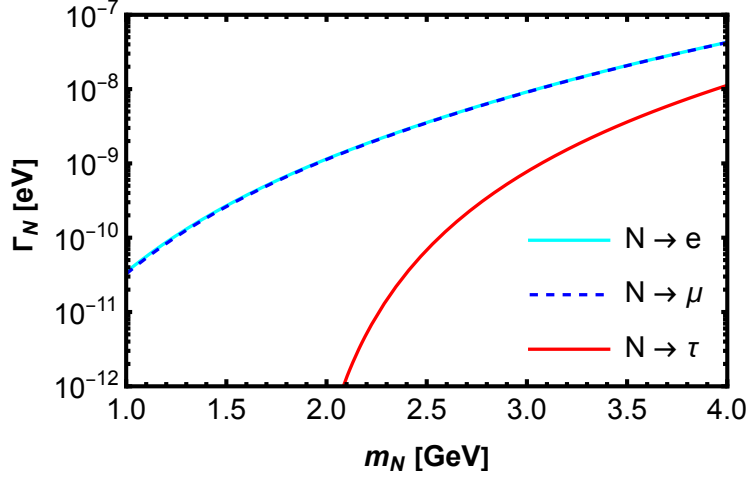


Figure 2. Decay width of an HSN into leptons. Here the notation $N \rightarrow \ell$ means the plotted line is the sum of all partial widths associated with the tagging lepton i.e. $\Gamma(N \rightarrow e) = \sum_{\ell} \Gamma(N \rightarrow e\bar{\ell}\nu_{\ell})$. For all three channels the mixing angle is chosen as $V_{N\ell} = 10^{-3}$.

Here $m_{i,j}$ are quark masses and q is the momentum of the gauge boson. In our case of the hadronic charged current q_i and q_j are up-type and down-type quarks, respectively. In the last line above the correlators have been decomposed into their transverse and longitudinal components

$$\Pi_{ij,V/A}^{(1)}(q^2) = -\frac{\Pi_{ij,V/A}^{[1]}(q^2)}{q^2}, \quad \Pi_{ij,V/A}^{(0)}(q^2) = \Pi_{ij,V/A}^{[2]}(q^2) + \frac{\Pi_{ij,V/A}^{[1]}(q^2)}{q^2}. \quad (2.6)$$

In studies of τ decays one commonly adopts the definition [20]

$$\Pi_{ij,V/A}^{(1+0)}(q^2) \equiv \Pi_{ij,V/A}^{(1)}(q^2) + \Pi_{ij,V/A}^{(0)}(q^2). \quad (2.7)$$

The correlators $\Pi^{[1]}$ and $\Pi^{[2]}$ are related to each other via a Ward identity [22, 23]

$$q^\mu q^\nu \Pi_{\mu\nu,ij}^{V/A} = q^4 \Pi_{ij,V/A}^{(0)} = (m_j \mp m_i)^2 \Pi_{ij}^{S/P} + (m_j \mp m_i) \langle 0 | \bar{q}_j q_j \mp \bar{q}_i q_i | 0 \rangle. \quad (2.8)$$

This identity connects the longitudinal part of the V or A correlator to the scalar or pseudo-scalar correlators $\Pi_{ij}^{S/P}$, respectively, where

$$\Pi_{ij}^{S/P}(q) = i \int dx e^{iqx} \langle 0 | \hat{T} \{ j_{ij}^{S/P}(x) j_{ij}^{S/P\dagger}(0) \} | 0 \rangle, \quad j_{ij}^{S/P} = \bar{q}_i(\gamma_5)q_j, \quad (2.9)$$

and the last term in Eq. (2.8) is the quark condensate. Thus in the chiral limit

$$\Pi_{ij,V/A}^{(0)} = 0. \quad (2.10)$$

For the W boson there are only contributions to the correlator by so-called non-singlet diagrams as seen in Fig. 3. Non-singlet diagrams only have cuts through at

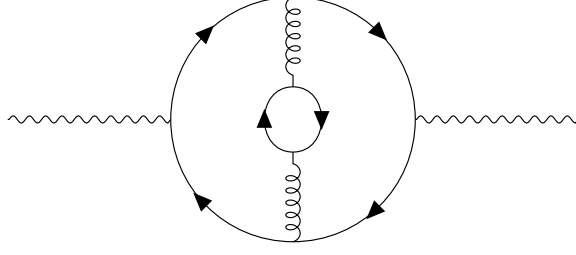


Figure 3. Sample non-singlet diagram to $\mathcal{O}(\alpha_s^2)$.

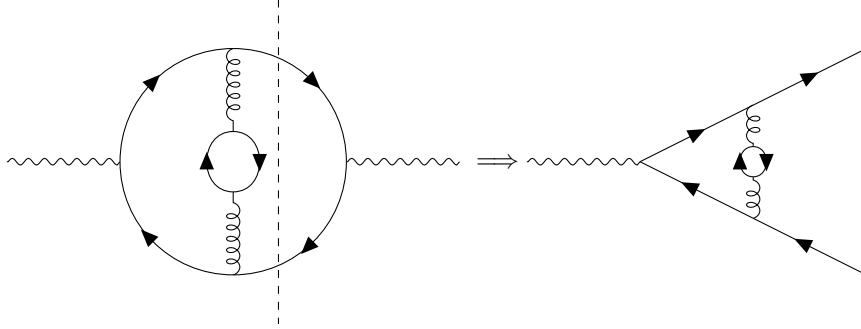


Figure 4. One possible cut of the loop diagram in Fig. 3. This corresponds to the decay amplitude $W \rightarrow q\bar{q}$ at $\mathcal{O}(\alpha_s^2)$ interfering with the tree-level amplitude.

least two fermion lines. Cuts indicate individual contributions to the imaginary part of a loop diagram with the particles on the cut line being on-shell (see. Fig. 4). From now on we adopt the chiral limit with zero quark masses. The applicability of perturbative QCD requires $q^2 \gg m_i^2$, which is certainly fulfilled for the three lightest quarks for $m_N \gtrsim 1$ GeV. If one of the final state quarks is c or b , there is a range of q^2 for which the c or b quark mass is non-negligible and can be included in an expansion in terms of $m_{c,b}^2/q^2$. These mass corrections are beyond the scope of this paper, i.e. for heavy hadrons our formulae are only valid for HSN decays with q^2 large enough that m_c or m_b can be set to zero i.e. $m_b^2 > q^2 \gg m_c^2$ or $q^2 \gg m_b^2$.

The correlators may be expressed as a series in

$$a_\mu = \frac{\alpha_s(\mu)}{\pi}, \quad (2.11)$$

where the coefficients are functions of the logarithm $\ln(-s/\mu^2)$ with $s = q^2$ the invariant mass of the hadronic state and the logarithm evaluated below the branch cut according to the Feynman prescription $s \rightarrow s + i\delta$, so that $\text{Im} \ln(-s/\mu^2 - i\delta) = \ln(s/\mu^2) - i\pi$. Since the longitudinal part of the correlator is proportional to the square of the quark mass it will not contribute in the chiral limit (see Eq. (2.8)). The sum of the longitudinal and transverse part of the correlator is given by [11]

$$\Pi_{ij, V/A}^{(1+0)}(s) = -\frac{1}{12\pi^2} \sum_{n=0}^{\infty} a_{\mu}^n \sum_{k=0}^{n+1} c_{n,k} \ln^k \left(\frac{-s}{\mu^2} \right), \quad (2.12)$$

and the coefficients $c_{n,1}$ are given by [10, 19, 20, 24–30]

$$c_{0,1} = c_{1,1} = 1, \quad (2.13)$$

$$c_{2,1} = -\left(\frac{11}{12} - \frac{2}{3}\zeta_3 \right) n_f + \frac{365}{24} - 11\zeta_3, \quad (2.14)$$

$$c_{3,1} = \left(\frac{151}{162} - \frac{19}{27}\zeta_3 \right) n_f^2 - \left(\frac{7847}{216} - \frac{262}{9}\zeta_3 + \frac{25}{9}\zeta_5 \right) n_f + \frac{87029}{288} - \frac{1103}{4}\zeta_3 + \frac{275}{6}\zeta_5, \quad (2.15)$$

$$c_{4,1} = \left(\frac{203}{324}\zeta_3 + \frac{5}{18}\zeta_5 - \frac{6131}{5832} \right) n_f^3 + \left(-\frac{40655}{864}\zeta_3 + \frac{5}{6}\zeta_3^2 - \frac{260}{27}\zeta_5 + \frac{1045381}{15552} \right) n_f^2 + \left(\frac{12205}{12}\zeta_3 - 55\zeta(3)^2 + \frac{29675}{432}\zeta_5 + \frac{665}{72}\zeta_7 - \frac{13044007}{10368} \right) n_f - \frac{7315}{48}\zeta_7 + \frac{65945}{288}\zeta_5 + \frac{5445}{8}\zeta_3^2 - \frac{5693495}{864}\zeta_3 + \frac{144939499}{20736}. \quad (2.16)$$

Here n_f denotes the number of active flavours and $\zeta_n \equiv \zeta(n)$ are values of the Riemann ζ -function. To reconstruct the remaining coefficients $c_{n,k}$ we can use the renormalization group (RG) equation. To this end, one considers the Adler function [31]

$$D^{(1+0)}(s) = -s \frac{d}{ds} \Pi_{ij, V/A}^{(1+0)}(s), \quad (2.17)$$

which is a physical object and μ -independent. Employing

$$\mu^2 \frac{d}{d\mu^2} D_{ij, V/A}^{(1+0)}(s) = 0, \quad (2.18)$$

one finds [11]

$$c_{2,2} = -\frac{\beta_0}{2} c_{1,1} \quad (2.19)$$

$$c_{3,3} = \frac{\beta_0^2}{3} c_{1,1}, \quad c_{3,2} = -\frac{\beta_1}{2} c_{1,1} - \beta_0 c_{2,1} \quad (2.20)$$

$$c_{4,4} = -\frac{\beta_0^3}{4} c_{1,1}, \quad c_{4,3} = \frac{5}{6} \beta_1 \beta_0 c_{1,1} + \beta_0^2 c_{2,1}, \quad (2.21)$$

$$c_{4,2} = -\frac{1}{2} (\beta_2 c_{1,1} + 2\beta_1 c_{2,1} + 3\beta_0 c_{3,1}),$$

where $c_{n,k} = 0$ if $k > n$ and $n \neq 0$ and the coefficients β_i of the QCD beta function are listed in Appendix A.

3 QCD Corrections to Charged Current HSN Decays

Using the correlator in Eq. (2.12) the differential inclusive decay rate of a HSN via a charged current reads

$$\begin{aligned} \frac{d\Gamma(N \rightarrow \ell X)}{ds} = & N_c \frac{G_F^2 m_N^5 |V_{N\ell}|^2}{192\pi^3} \times \frac{12\pi}{m_N^2} \left(1 + x_\ell^2 - \frac{s}{m_N^2}\right) \sqrt{\lambda\left(1, \frac{s}{m_N^2}, x_\ell^2\right)} \\ & \times \left[\left(1 + 2\frac{s}{m_N^2} + x_\ell^2 - \frac{4x_\ell^2}{1 + x_\ell^2 - \frac{s}{m_N^2}}\right) \text{Im}\Pi^{(1+0)}(s) - 2\frac{s}{m_N^2} \text{Im}\Pi^{(0)}(s) \right], \end{aligned} \quad (3.1)$$

integrating over s , or the dimensionless variable $x = s/m_N^2$, leads to

$$\begin{aligned} \Gamma(N \rightarrow \ell X) = & N_c \frac{G_F^2 m_N^5 |V_{N\ell}|^2}{192\pi^3} \times 12\pi \int_0^{(1-x_\ell)^2} dx (1 + x_\ell^2 - x) \sqrt{\lambda(1, x, x_\ell^2)} \\ & \times \left[\left(1 + 2x + x_\ell^2 - \frac{4x_\ell^2}{1 + x_\ell^2 - x}\right) \text{Im}\Pi^{(1+0)}(m_N^2 x) - 2x \text{Im}\Pi^{(0)}(m_N^2 x) \right], \end{aligned} \quad (3.2)$$

with $x_\ell = m_\ell/m_N$ and where we used

$$\begin{aligned} \Pi^{(J)} = & |V_{ud}|^2 \left(\Pi_{ud,V}^{(J)} + \Pi_{ud,A}^{(J)} \right) + |V_{us}|^2 \left(\Pi_{us,V}^{(J)} + \Pi_{us,A}^{(J)} \right) + \dots \\ = & 2(|V_{ud}|^2 + |V_{us}|^2 + \dots) \Pi_V^{(J)}, \end{aligned} \quad (3.3)$$

since the vector and axial vector contribution are equal in magnitude. Here the dots indicate to the inclusion of heavier mesons i.e. D or B mesons. Since $\Pi^{(0)} \sim m_q^2$ we neglect it. The integration region with small x involves hadronic resonances while the integrand in Eq. (3.2) is smooth. Eq. (3.2) nevertheless reproduces the correct result as can be derived from analyticity properties of $\Pi^{(J)}$, see Appendix B for details.

Choosing $\mu = m_N$ the imaginary part of the correlator reads

$$\begin{aligned} \text{Im}\Pi_V^{(1+0)}(m_N^2 x) = & -\frac{1}{12\pi^2} \sum_{n=0}^{\infty} a_{m_N}^n \sum_{k=0}^{n+1} c_{n,k} \text{Im} \ln^k(-x) \\ = & \frac{1}{12\pi} \left\{ 1 + a_{m_N} + a_{m_N}^2 (c_{2,1} + 2c_{2,2} \ln(x)) \right. \\ & + a_{m_N}^3 (c_{3,1} + 2c_{3,2} \ln(x) - (\pi^2 - 3\ln^2(x))c_{3,3}) \\ & + a_{m_N}^4 (c_{4,1} + 2c_{4,2} \ln(x) - (\pi^2 - 3\ln^2(x))c_{4,3} \\ & \left. - (4\pi^2 \ln(x) - 4\ln^3(x))c_{4,4}) \right\} \end{aligned} \quad (3.4)$$

and leads to integrals of the form

$$I_k = \int_0^{(1-x_\ell)^2} dx \left((1 + x_\ell^2 - x)(1 + 2x + x_\ell^2) - 4x_\ell^2 \right) \sqrt{\lambda(1, x, x_\ell^2)} \ln^k(x), \quad (3.5)$$

Up to $k = 2$ the integrals are analytically calculable in terms of dilogarithm and trilogarithm functions:

$$I_0 = \frac{1}{2} \left(1 - 8x_\ell^2 + 8x_\ell^6 - x_\ell^8 - 12x_\ell^4 \ln(x_\ell^2) \right), \quad (3.6)$$

$$\begin{aligned} I_1 = & -\frac{19}{24} + \frac{13}{3}x_\ell^2 - 12\zeta_2 x_\ell^4 - \frac{13}{3}x_\ell^6 + \frac{19}{24}x_\ell^8 \\ & + \left(-3x_\ell^4 - 4x_\ell^6 + \frac{1}{2}x_\ell^8 \right) \ln(x_\ell^2) \\ & + \left(1 - 8x_\ell^2 + 8x_\ell^6 - x_\ell^8 \right) \ln(1 - x_\ell^2) + 12x_\ell^4 \text{Li}_2(x_\ell^2), \end{aligned} \quad (3.7)$$

$$\begin{aligned} I_2 = & \frac{265}{144} - \frac{151}{18}x_\ell^2 - 12(\zeta_2 + 2\zeta_3)x_\ell^4 + \left(\frac{151}{18} - 16\zeta_2 \right)x_\ell^6 + \left(-\frac{265}{144} + 2\zeta_2 \right)x_\ell^8 \\ & + \left(-\frac{19}{6} + \frac{52}{3}x_\ell^2 - 48\zeta_2 x_\ell^4 - \frac{52}{3}x_\ell^6 + \frac{19}{6}x_\ell^8 + 48x_\ell^4 \text{Li}_2(x_\ell^2) \right) \ln(1 - x_\ell^2) \\ & + (2 - 16x_\ell^2 + 16x_\ell^6 - 2x_\ell^8) \ln^2(1 - x_\ell^2) \\ & + \left(-x_\ell^2 + \frac{15}{2}x_\ell^4 + \frac{23}{3}x_\ell^6 - \frac{19}{12}x_\ell^8 \right. \\ & \quad \left. + (-1 + 8x_\ell^2 - 8x_\ell^6 + x_\ell^8) \ln(1 - x_\ell^2) + 24x_\ell^4 \ln^2(1 - x_\ell^2) - 12x_\ell^4 \text{Li}_2(x_\ell^2) \right) \ln(x_\ell^2) \\ & + (-1 + 8x_\ell^2 + 12x_\ell^4 + 8x_\ell^6 - x_\ell^8) \text{Li}_2(x_\ell^2) \\ & + 24x_\ell^4 \text{Li}_3(x_\ell^2) + 48x_\ell^4 \text{Li}_3(1 - x_\ell^2). \end{aligned} \quad (3.8)$$

In Appendix C we give approximations to these integrals for easier use.

We next derive a new analytical result holding as well for $k \geq 3$, defined in terms of a well converging sum. To do this we first use the following series representation of the square root of the Källén function,

$$\begin{aligned} \frac{d^n}{dx^n} \sqrt{\lambda(1, x, x_\ell^2)} = & \sum_j^{\lfloor \frac{n}{2} \rfloor} (-1)^{n-j} \left(-\frac{1}{2} \right)_{n-j} (2j-1)!! \binom{n}{2j} \\ & \times \frac{\left(\lambda'(1, x, x_\ell^2) \right)^{n-2j} \left(\lambda''(1, x, x_\ell^2) \right)^j}{\left(\lambda(1, x, x_\ell^2) \right)^{\frac{2(n-j)-1}{2}}}, \end{aligned} \quad (3.9)$$

where $(a)_n = a(a+1)(a+2) \cdots (a+n-1)$ is the Pochhammer symbol, $\lfloor j \rfloor$ is the

floor function and

$$\lambda(1, x, x_\ell^2) = x^2 - 2x(1 - x_\ell^2) + (1 - x_\ell^2)^2, \quad (3.10)$$

$$\lambda'(1, x, x_\ell^2) = \frac{d\lambda(1, x, x_\ell^2)}{dx} = 2x - 2(1 - x_\ell^2), \quad (3.11)$$

$$\lambda''(1, x, x_\ell^2) = \frac{d^2\lambda(1, x, x_\ell^2)}{dx^2} = 2. \quad (3.12)$$

We write

$$I_k(x_\ell^2, a) = \sum_{n=0}^{\infty} \frac{1}{n!} A_n(x_\ell^2) B_{n,k}(x_\ell^2, a) \quad (3.13)$$

with

$$\begin{aligned} A_n(x_\ell^2) &\equiv \left. \frac{d^n}{dx^n} \sqrt{\lambda(1, x, x_\ell^2)} \right|_{x=0} \\ &= \sum_j^{\lfloor \frac{n}{2} \rfloor} (-1)^{n-j} \left(-\frac{1}{2} \right)_{n-j} (2j-1)!! \binom{n}{2j} 2^{n-j} (1 - x_\ell^2)^{1-n}, \end{aligned}$$

and

$$\begin{aligned} B_{n,k}(x_\ell^2, a) &\equiv \int_0^a dx \left((1 + x_\ell^2 - x)(1 + 2x + x_\ell^2) - 4x_\ell^2 \right) x^n \ln^k(x) \\ &= -2I_{n+2,k}(a) + (1 + x_\ell^2)I_{n+1,k}(a) + (1 - x_\ell^2)^2 I_{n,k}(a). \end{aligned} \quad (3.14)$$

The integrals in this expression are given by

$$\begin{aligned} I_{n,k}(a) &\equiv \int_0^a dx x^n \ln^k x \\ &= a^{n+1} \sum_{l=0}^k (-k)_l (n+1)^{-l-1} \ln^{k-l} a, \end{aligned} \quad (3.15)$$

which completes the calculation of I_k in Eq. (3.5).

Inserting Eq. (3.4) into Eq. (3.2) and using Eq. (3.5) finally gives the full semi-

hadronic width for decays of sterile neutrinos lighter than the D^+ meson

$$\begin{aligned}
\Gamma(N \rightarrow \ell X) = & N_c \frac{G_F^2 m_N^5 |V_{N\ell}|^2}{192\pi^3} \cdot 2(|V_{ud}|^2 + |V_{us}|^2) \\
& \times \left[I_0(x_\ell^2, (1-x_\ell)^2) c_{0,1} + a_{m_N} c_{1,1} I_0(x_\ell^2, (1-x_\ell)^2) \right. \\
& + a_{m_N}^2 [c_{2,1} I_0(x_\ell^2, (1-x_\ell)^2) + 2c_{2,2} I_1(x_\ell^2, (1-x_\ell)^2)] \\
& + a_{m_N}^3 [c_{3,1} I_0(x_\ell^2, (1-x_\ell)^2) + 2c_{3,2} I_1(x_\ell^2, (1-x_\ell)^2) \\
& \quad - (\pi^2 I_0(x_\ell^2, (1-x_\ell)^2) - 3I_2(x_\ell^2, (1-x_\ell)^2)) c_{3,3}] \\
& + a_{m_N}^4 [c_{4,1} I_0(x_\ell^2, (1-x_\ell)^2) + 2c_{4,2} I_1(x_\ell^2, (1-x_\ell)^2) \\
& \quad - (\pi^2 I_0(x_\ell^2, (1-x_\ell)^2) - 3I_2(x_\ell^2, (1-x_\ell)^2)) c_{4,3} \\
& \quad \left. - (4\pi^2 I_1(x_\ell^2, (1-x_\ell)^2) - 4I_3(x_\ell^2, (1-x_\ell)^2)) c_{4,4} \right].
\end{aligned} \tag{3.16}$$

Logarithms involving the renormalization scale may be reconstructed by using the relation in Appendix A. Sterile neutrinos heavier than the D^+ meson also obey the relation above once the corresponding CKM element as well as threshold effects are included.

Additionally we also calculated the integral in Eq. (3.5) for an arbitrary upper limit of the hadronic invariant mass, to allow calculating the integrated spectrum of the decay

$$\Gamma_{\text{cut}}(N \rightarrow \ell X) = \int_0^{s_{\text{max}}} ds \frac{d\Gamma(N \rightarrow \ell X)}{ds}, \quad s_{\text{max}} \in [\mathcal{O}(1 \text{ GeV}), (m_N - m_\ell)^2], \tag{3.17}$$

$$= \int_0^{x_{\text{max}}} dx \frac{d\Gamma(N \rightarrow \ell X)}{dx} \tag{3.18}$$

where we defined $x_{\text{max}} = s_{\text{max}}/m_N^2$. $\Gamma_{\text{cut}}(N \rightarrow \ell X)$ obeys Eq. (3.16) with $I_k = I_k(x_\ell^2, x_{\text{max}})$. Up to $k = 2$ we found a closed analytical form of the $I_k(x_\ell^2, x_{\text{max}})$. The expressions are found in Appendix D, but the calculation from Eq. (3.13) is more easy even for $k \leq 2$.

4 Numerical Analysis

4.1 Quality of the perturbation series

Perturbative QCD describes observables in an expansion of the strong coupling constant accurately if the relevant energy scale μ is large enough such that α_s is small. Any observable O_μ at the scale μ may be written as

$$O_\mu = \sum_n r_n \alpha_s(\mu)^n = r_0 + r_1 \alpha_s(\mu) + r_2 \alpha_s(\mu)^2 + \mathcal{O}(\alpha_s(\mu)^3). \tag{4.1}$$

However, at small scales ($\mu \sim \mathcal{O}(1 \text{ GeV})$) the strong coupling constant becomes large and an expansion in α_s is no longer guaranteed to converge. For the τ lepton with a mass of $m_\tau = 1.776 \text{ GeV}$ it was only possible to correctly describe the inclusive hadronic decay width through the inclusion of five-loop corrections. Only at the five-loop level does the perturbative description become stable i.e. the $\mathcal{O}(\alpha_s^4)$ corrections lead to a significantly reduced dependence on the renormalization scale [10]. In the case of a HSN with mass comparable to the τ the kinematics is, up to the mass of the lepton attached to the HSN, the same. Setting $m_\ell = 0$ leads to the same numerical coefficients as in τ decay

$$\frac{\Gamma(N \rightarrow \ell X)}{|V_{ud}|^2 + |V_{us}|^2} = N_c \frac{G_F^2 m_N^5 |V_{N\ell}|^2}{192\pi^3} \times \left[1 + a_{m_N} + 5.202a_{m_N}^2 + 26.366a_{m_N}^3 + 127.079a_{m_N}^4 \right], \quad (4.2)$$

perfectly agreeing with Ref. [10]. For a HSN mass around 3 GeV the inclusive semi-hadronic decay with $\ell = \tau$ in the final state is kinematically accessible. The lepton mass ratio is then sizable, $x_\tau = 0.592$, and

$$\frac{\Gamma(N \rightarrow \tau X)}{|V_{ud}|^2 + |V_{us}|^2} = N_c \frac{G_F^2 m_N^5 |V_{N\ell}|^2}{192\pi^3} \times 0.071 \left[1 + a_{m_N} + 8.376a_{m_N}^2 + 74.605a_{m_N}^3 + 669.805a_{m_N}^4 \right], \quad (4.3)$$

largely reducing the decay rate and making the convergence of the perturbative series worse.

In Fig. 5 we show the full decay width. The widths for $\ell = e$ and $\ell = \mu$ are indistinguishable. For $m_N \geq m_\mu + m_D$ the decay channel into charmed mesons opens up. For this reason we omit the region $m_N \in [m_\mu + m_D, 3 \text{ GeV}]$ in Fig. 5 as here there are resonances of charmed mesons. They are dominated by non-perturbative effects making an accurate perturbative description in this region impossible. We show the $\ell = \mu$ rate again beyond $m_N \geq 3 \text{ GeV}$. We have computed the error band by taking as uncertainty the difference between the minimal and maximal width with respect to the renormalization scale i.e. $\sigma_\Gamma = (\max \Gamma_N(\mu) - \min \Gamma_N(\mu))/2$ for $0.8 \text{ GeV} \leq \mu \leq 3.5 \text{ GeV}$. Since we did not include charm mass corrections we expect an additional error of $\mathcal{O}(m_D^2/q^2) = \mathcal{O}(40\%)$ for $m_N = 3 \text{ GeV}$, which is not shown. In Fig. 6 we plot the effect of each order in α_s on the total decay width for $\ell = \mu$. For small HSN masses, close to the kinematic threshold of multi-hadron production, we see that including more corrections in α_s does not improve the convergence. This is even more pronounced in Fig. 6(b) where the relative increase compared to the leading order is large for HSN masses in a window below $\sim 1 \text{ GeV}$. Beyond 1 GeV the perturbative behavior rapidly improves and higher order corrections become smaller with higher orders in α_s in relation to the leading order. We specifically analyzed

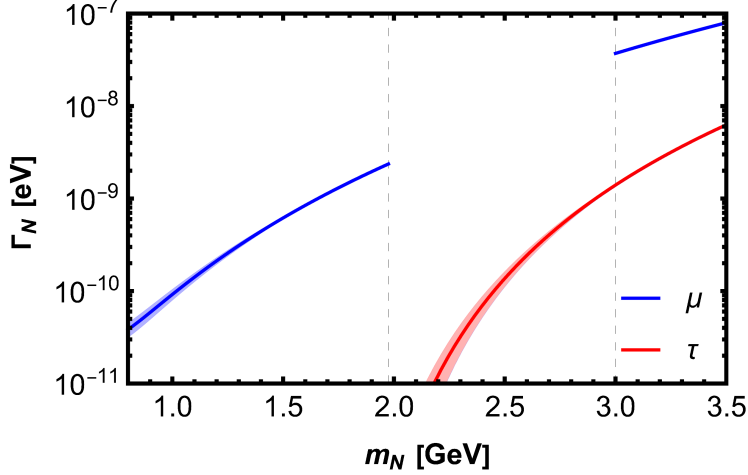


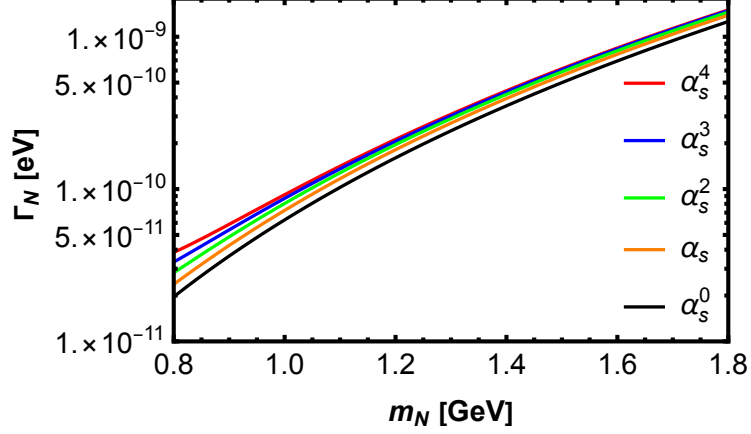
Figure 5. Hadronic decay widths $\Gamma(N \rightarrow \ell X)$ for the tagging leptons $\ell = \mu, \tau$ with a mixing angle of $V_{N\ell} = 10^{-3}$. The width for $\ell = e$ looks like the $\ell = \mu$ width. The numerics of the running coupling were calculated with the help of RunDec [32, 33]. We do not show the region $m_N \in [m_\mu + m_D, 3 \text{ GeV}]$ where we expect large non-perturbative effects. The error band is taken as the difference between minimum and maximum of the width with respect to the renormalization scale $\sigma_\Gamma = (\max \Gamma_N(\mu) - \min \Gamma_N(\mu))/2$ for $0.8 \text{ GeV} \leq \mu \leq 3.5 \text{ GeV}$. We do not include the uncertainty from our omission of quark masses, which can be sizable, $\mathcal{O}(m_D^2/q^2) = \mathcal{O}(40\%)$ for $m_N = 3 \text{ GeV}$, beyond the charm production threshold.

the scale dependence of the widths by expressing a_{m_N} in terms of logarithms of the renormalization scale μ and the HSN mass as seen in Appendix A. In Fig. 7 the scale dependence for different HSN masses is shown. The scale dependence is very strong close to the kinematic threshold. Increasing the mass of the HSN the scale dependence reduces. We see that HSN masses around 1.5 GeV, including the highest order corrections in α_s available, lead to a flat scale dependence.

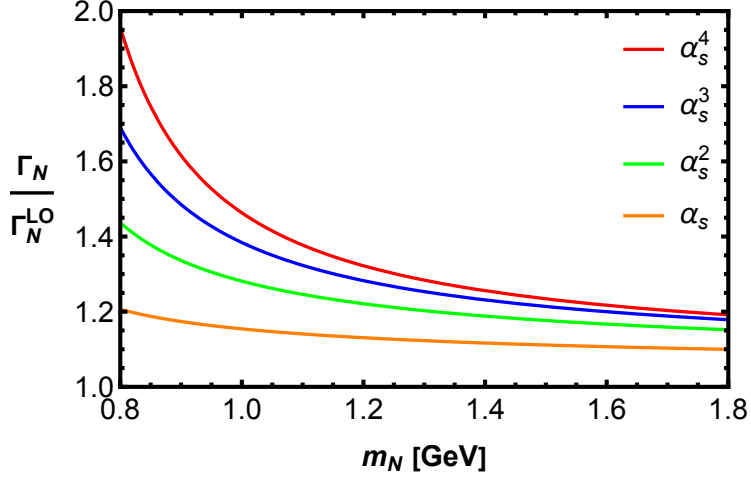
In the $\ell = \tau$ final state lepton case the discussion is qualitatively similar to the $\ell = e$ and $\ell = \mu$ case. Looking only at the decay width in Fig. 8(a) the effect of poor convergence does not seem to be as pronounced, however, in absolute values it is comparable to the decay into a muon as seen in Fig. 8(b). As in the muon case, the quality of the perturbative series rapidly increases for larger HSN masses. In Fig. 9 the scale dependence for different HSN masses is shown. The scale dependence reduces for larger masses. At a HSN mass of 3 GeV the $\mathcal{O}(\alpha_s^4)$ corrections reduce the scale dependence significantly. For larger HSN masses already lower orders results show a satisfactory small scale dependence.

4.2 Branching ratios of HSN

Without the neutral current contributions mediated by the Z boson one cannot calculate the total width, which is needed for branching ratio predictions. However



(a) Inclusive HSN decay width with $\ell = \mu$. Here $V_{N\ell=\mu} = 10^{-3}$.



(b) Γ_N at different orders of α_s , normalised to the LO result.

Figure 6. Inclusive decay width $\Gamma_N = \Gamma(N \rightarrow \mu X)$ as a function of m_N .

ratios of branching ratios for the charged decays can be calculated

$$\kappa_\ell^P = \frac{Br(N \rightarrow \ell P)}{Br(N \rightarrow \ell X)} = \frac{\Gamma(N \rightarrow \ell P)}{\Gamma(N \rightarrow \ell X)}, \quad (4.4)$$

here $P = \pi^+, K^+, D^+, \dots$ is some meson, $\Gamma(N \rightarrow \ell P)$ is the width of a HSN into a meson

$$\Gamma(N \rightarrow \ell P) = \frac{G_F^2 m_N^3 |V_{N\ell}|^2}{16\pi} |V_{u'd'}|^2 f_P^2 \left[(1 - x_\ell^2)^2 - x_P^2 (1 + x_\ell^2) \right] \sqrt{\lambda(1, x_\ell^2, x_P^2)}, \quad (4.5)$$

where f_P is the meson decay constant, $|V_{u'd'}|$ is the relevant CKM matrix element, and $x_i = m_i/m_N$, and $\Gamma(N \rightarrow \ell X)$ is the fully inclusive semi-hadronic decay rate as given in Eq. (3.16). For our predictions of κ_ℓ^P we assume $m_N > 1.5$ GeV for electron and muon tagging and $m_N > 3$ GeV for tau tagging. In Fig. 10 the κ -ratio for muon

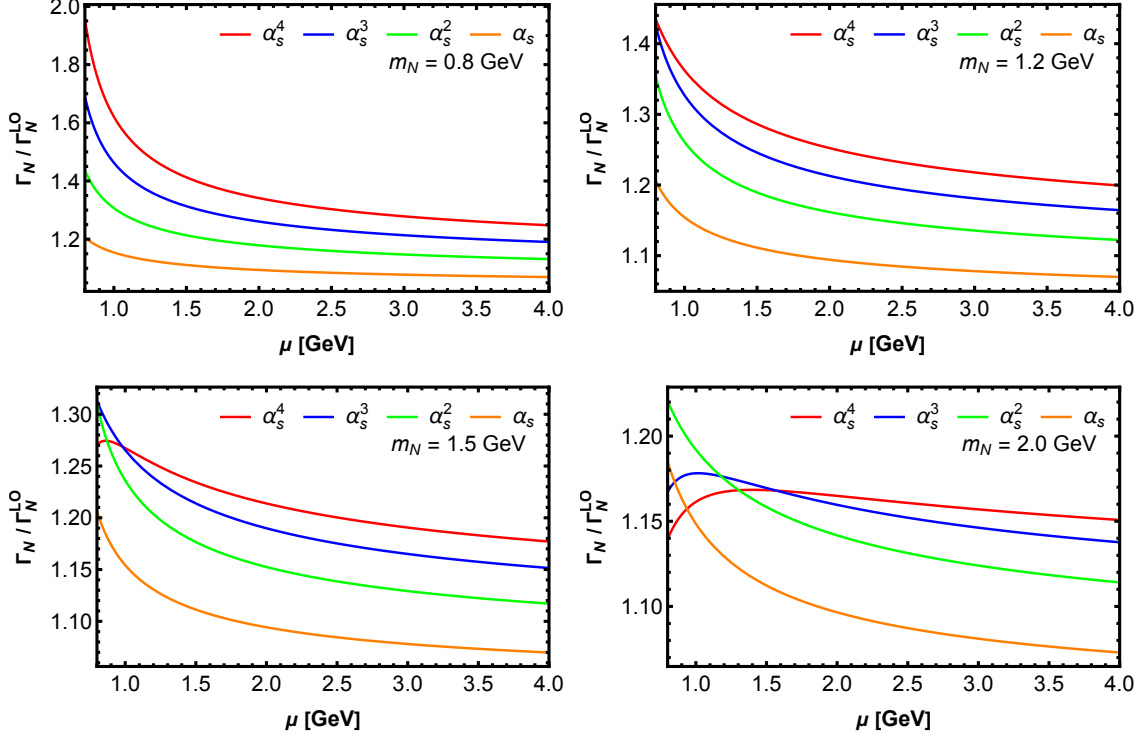


Figure 7. Scale dependence of the inclusive decay width $\Gamma_N = \Gamma(N \rightarrow \mu X)$ for different HSN masses.

and tau tagging are shown. In both cases pions dominate the decay and only a few CKM-suppressed decays to kaons are predicted. For this reason we omit decays to D mesons as they are more suppressed than those into kaons due to the smaller phase space. In addition we also show the impact of the inclusion of D_s mesons. D_s mesons are produced copiously beyond the charm threshold as $V_{cs} \approx 1$. We exclude the region $m_N \in [m_\mu + m_D, 3 \text{ GeV}]$ as here non-perturbative charm resonance effects dominate the width. As long as the decay channels to charmed final states are absent, at least 12% of the charged-current decays of HSN are $N \rightarrow \ell \pi$ for all considered values of m_N .

4.3 Constraints on $\theta_{N\tau}$ from the τ lifetime

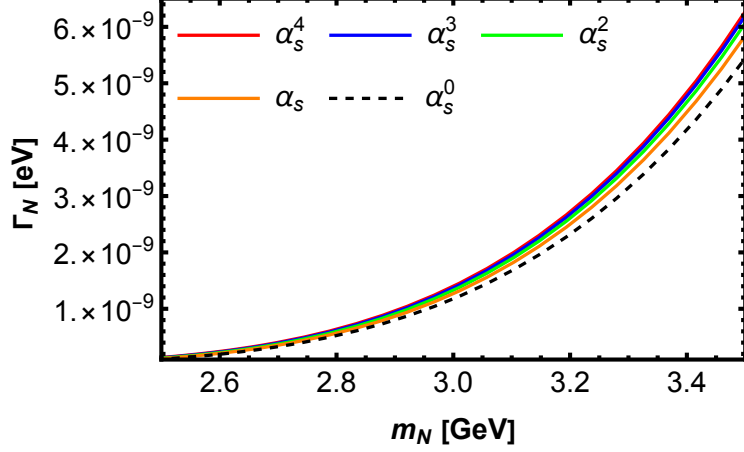
The current world average of the τ -lifetime

$$\tau_\tau^{\text{exp.}} = (290.29 \pm 0.53) \text{ fs} \quad [38] \quad (4.6)$$

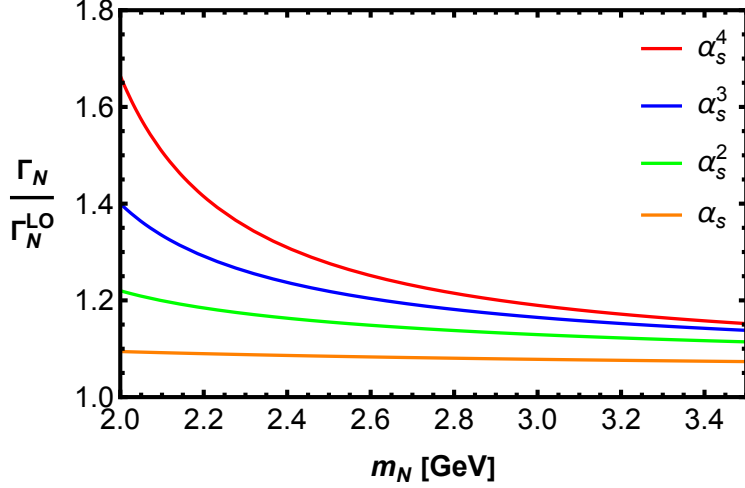
agrees with the SM theory prediction

$$\tau_\tau^{\text{SM}} = (288.59 \pm 2.31) \text{ fs} \quad [37, 39]. \quad (4.7)$$

Whenever a sterile neutrino interaction is present it comes with a factor of the mixing angle $V_{N\tau} = \sin \theta_{N\tau}$. At the same time SM neutrino interactions receive a



(a) Inclusive HSN decay width with $\ell = \tau$. Here $V_{N\ell=\tau} = 10^{-3}$.



(b) Γ_N at different orders of α_s , normalised to the LO result.

Figure 8. Inclusive decay width $\Gamma_N = \Gamma(N \rightarrow \tau X)$

contribution involving $\cos \theta_{N\tau}$. Mixing is possible between one or more generations of SM neutrinos. If there is mixing with ν_e or ν_μ this has an impact on the Fermi constant. A complete analysis including also mixing with e or μ requires a full electroweak fit (see Ref.[40]) and is beyond the scope of this work. Hence we only look at mixing with ν_τ , and define $\theta \equiv \theta_{N\tau}$. Then a sterile neutrino will modify the total width, implying the following constraint on θ :

$$\tau_\tau^{\text{exp.}} = \frac{1 - \mathcal{B}_\tau^s}{\cos^2 \theta (1 - \mathcal{B}_\tau^s) \Gamma^\text{SM} + \sin^2 \theta \Gamma^N}, \quad (4.8)$$

where $\mathcal{B}_\tau^s = 0.0292$ [37] is the branching fraction of τ decays into strange final states, $(1 - \mathcal{B}_\tau^s) \Gamma^\text{SM}$ is the SM width involving leptonic and non-strange hadronic decays, and Γ^N is the sterile neutrino contribution i.e. $\tau \rightarrow NX$. Γ^SM is calculated as

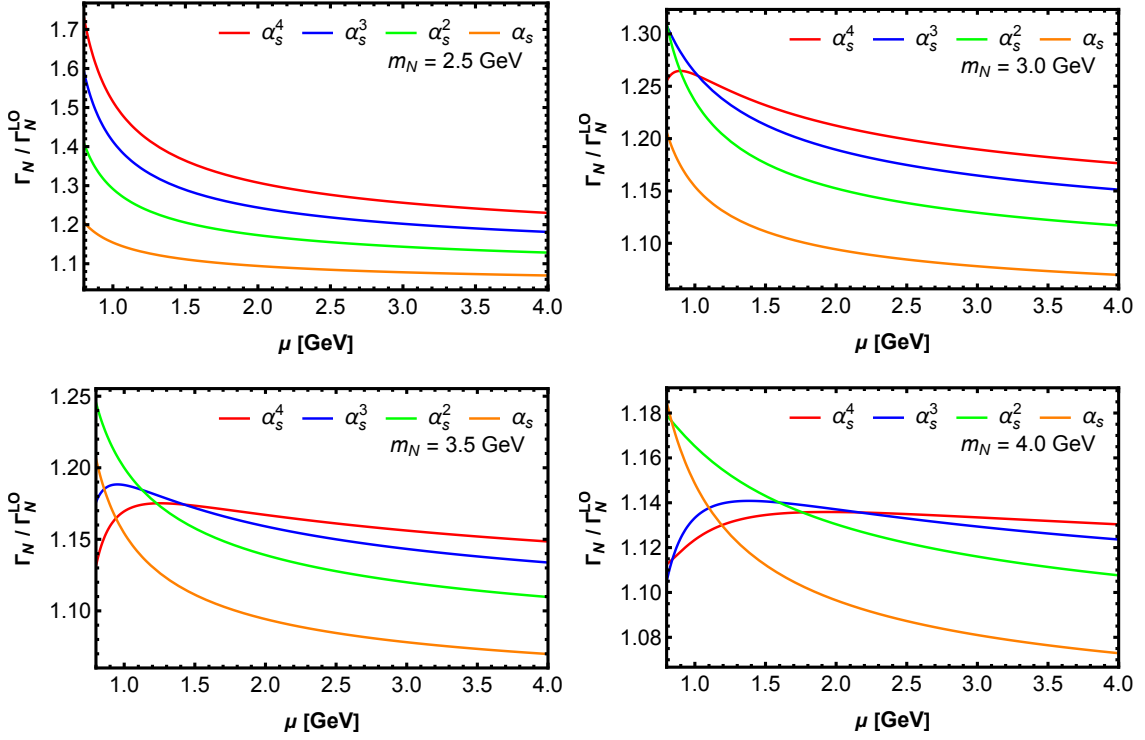
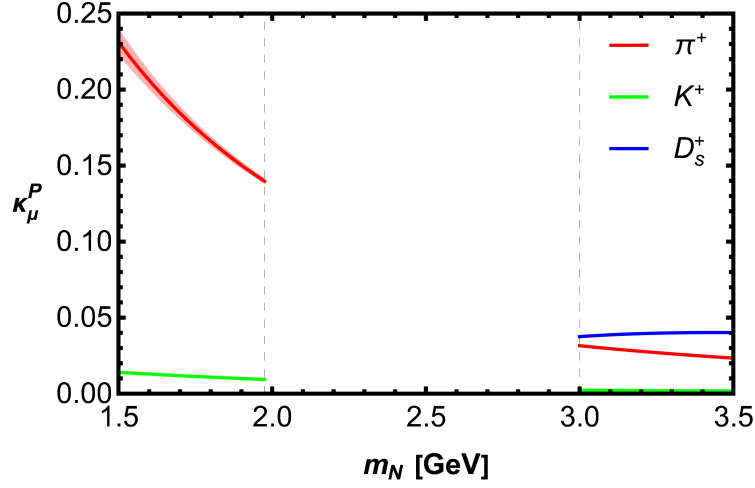


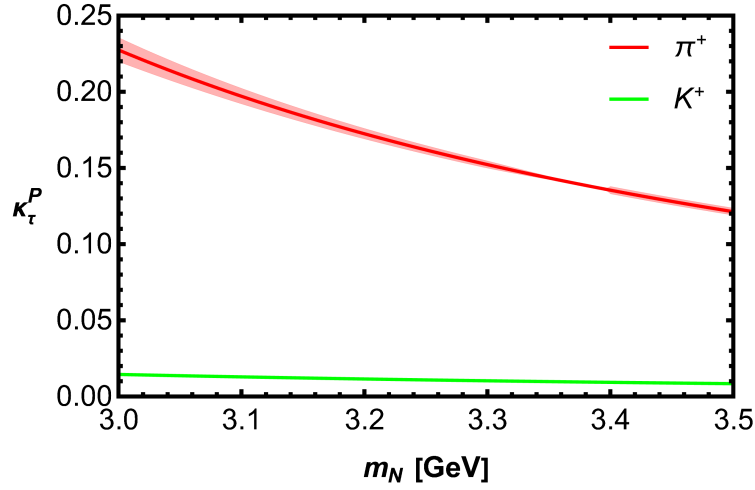
Figure 9. Scale dependence of the inclusive decay width $\Gamma_N = \Gamma(N \rightarrow \tau X)$ for different HSN masses.

$\Gamma^{\text{SM}} = 1/\tau_\tau^{\text{SM}}$ and Γ^N follows from Eq. (3.16) by replacing $V_{N\ell} \rightarrow 1$, $V_{us} \rightarrow 0$, $m_N \rightarrow m_\tau$, and $I_k(x_\ell^2, (1-x_\ell)^2) \rightarrow I_k(m_N^2/m_\tau^2, (1-m_N/m_\tau)^2)$. For the strong coupling constant we use $\alpha_s^{n_f=3}(m_\tau) = 0.316$ which we obtain by using the weighted average $\alpha_s^{n_f=5}(M_Z) = 0.1182$ of all measurements listed in the PDG [37], except the one using τ decay, and running $\alpha_s(M_Z)$ down to m_τ . In Fig. 11 we show the renormalization scale dependence of the τ decay width. At $\mathcal{O}(\alpha_s^4)$ the scale dependence remains sufficiently flat up to HSN masses around $m_N = 600$ MeV. For larger HSN masses the perturbative description becomes poorer.

Sterile neutrinos solely produced through mixing with ν_τ will always decrease the τ width and thus prolong the predicted lifetime, possibly bringing it into tension with the experimental value. This is so, because the decay rate to ν_τ is decreased by a factor of $\cos^2 \theta_{N\tau}$ while the additional decay channel with N , proportional to $\sin^2 \theta_{N\tau}$ involves phase-space suppression. Neglecting electroweak corrections in Γ^N we use Eq. (4.8) to determine the parameter space for θ and m_N in agreement with the measured τ lifetime, see Fig. 12, which shows the 1σ region of the allowed mixing angle and HSN mass, up to $m_N \leq 600$ MeV. We further show the allowed region when the experimental value in Eq. (4.6) is varied in the 3σ range, while we do not triple the theoretical uncertainty. For $m_N > 600$ MeV we continue our 1σ and 3σ lines for illustration, bearing in mind that the quality of the perturbative calculation



(a) κ_μ^P



(b) κ_τ^P

Figure 10. $N \rightarrow \ell P$ branching fractions (normalized to $Br(N \rightarrow \ell N)$) for $P = \pi^+, K^+, D_s^+$, see Eq. (4.4). We use $f_D = (212.0 \pm 0.7) \text{ MeV}$, $f_{D_s} = (249.9 \pm 0.5) \text{ MeV}$ [34–36], and $|V_{cd}| = 0.221 \pm 0.004$, and $|V_{cs}| = 0.975 \pm 0.006$ [37]. The error bands are the same as in Fig. 5.

diminishes significantly for $m_N \gtrsim 600 \text{ MeV}$, while the perturbation series for the inclusive hadronic τ decay width converges well for $m_N \lesssim 600 \text{ MeV}$.

Eq. (4.8) holds for any value of m_N , in particular, it also holds for $m_N > m_\tau$. In this case $\Gamma_N = 0$ and Eq. (4.8) becomes

$$\sin^2 \theta = 1 - \frac{\tau_\tau^{\text{th.}}}{\tau_\tau^{\text{exp.}}} = 0.00586 \pm 0.00816, \quad (4.9)$$

which leads to

$$|\sin \theta| = (7.65 \pm 5.33) \cdot 10^{-2}. \quad (4.10)$$

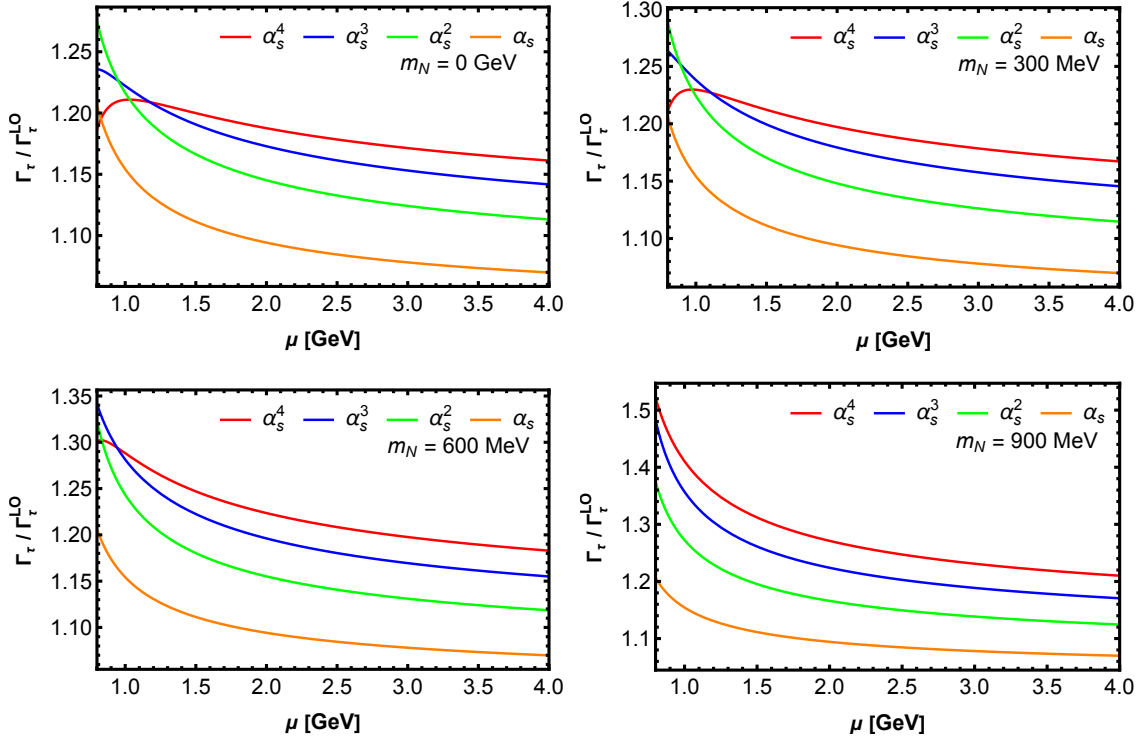


Figure 11. Scale dependence of the inclusive τ decay width with a final state HSN.

4.4 Contributions on $\theta_{N\tau}$ for $m_N > m_\tau$ from τ branching fractions

HSNs heavier than τ affect τ_τ in Eq. (4.8) indirectly through the cosine of the mixing angle. To study this scenario we look at the decays $\tau^- \rightarrow \pi^- \nu_\tau$, $\tau^- \rightarrow K^- \nu_\tau$, and $\tau \rightarrow \nu_\tau \ell \bar{\nu}_\ell$. This will allow us to bypass the theoretical uncertainty of the total hadronic width feeding into τ_τ in Eq. (4.7). The decay widths of interest read

$$\Gamma(\tau \rightarrow P \nu_\tau) = \cos^2 \theta \Gamma_{\text{SM}}(\tau \rightarrow P \nu_\tau) \quad (4.11)$$

$$= \frac{G_F^2 m_\tau^3 \cos^2 \theta}{16\pi} |V_{uq}|^2 f_P^2 \left(1 - \frac{m_P^2}{m_\tau^2}\right)^2 (1 + \delta_{\text{RC}}^{(P)}),$$

$$\begin{aligned} \Gamma(\tau \rightarrow \nu_\tau \ell \bar{\nu}_\ell) &= \cos^2 \theta \Gamma_{\text{SM}}(\tau \rightarrow \nu_\tau \ell \bar{\nu}_\ell) = \frac{G_F^2 m_\tau^5 \cos^2 \theta}{192\pi^3} \\ &\times \left[(1 - 8x_\ell^2 + 8x_\ell^6 - x_\ell^8 - 12x_\ell^4 \ln(x_\ell^2)) + \frac{\alpha(m_\tau)}{\pi} H_1 + \frac{\alpha^2(m_\tau)}{\pi^2} H_2 \right], \end{aligned} \quad (4.12)$$

where $x_\ell = m_\ell/m_\tau$, P is either K^- or π^- , f_P is the meson decay constant, and V_{uq} is the CKM matrix element. We have added the $\cos \theta$ factor to account for the effect of HSN mixing. Here the $\delta_{\text{RC}}^{(P)}$ are the radiative QED corrections governed by $\alpha(m_\tau)$. We use the values $\delta_{\text{RC}}^{(\pi)} = 0.0194 \pm 0.0061$ and $\delta_{\text{RC}}^{(K)} = 0.0204 \pm 0.0062$ [41]. The H_i

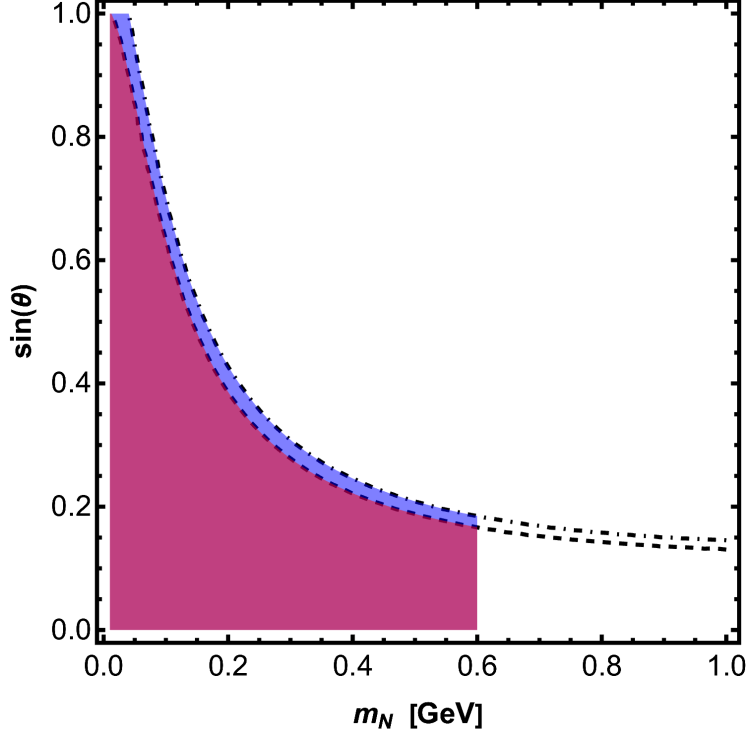


Figure 12. Allowed parameter space deduced from the measured τ lifetime in Eq. (4.6) via Eq. (4.8) at the 1σ (purple) and 3σ (purple and blue) levels. For $m_N \leq 600$ MeV we trust the perturbative calculation. The dashed lines for $m_N > 600$ MeV indicate the perturbative result in a region where the description is no longer reliable.

are the radiative QED corrections for leptonic decay, reading [42–46]

$$H_1 = \left(\frac{25}{8} - \frac{\pi^2}{2} \right) - (34 + 24 \ln x_\ell) x_\ell^2 + 16\pi^2 x_\ell^3 + \mathcal{O}(x_\ell^4) \quad (4.13)$$

$$H_2 = \frac{156815}{5184} - \frac{518}{81}\pi^2 - \frac{895}{36}\zeta_3 + \frac{67}{720}\pi^4 + \frac{53}{6}\pi^2 \ln 2 - (0.042 \pm 0.002) - \frac{15}{32}\pi^2 x_\ell + \mathcal{O}(x_\ell^2) \quad (4.14)$$

We use the measured τ lifetime $\tau_\tau = (290.29 \pm 0.53)$ fs [38], the branching ratios, decay constants, and parameters listed in Tab. 1. We have determined the pion decay constant from the ratio f_{K^+}/f_{π^+} and f_{K^+} .

This leads to the following mixing angles allowed by the experimental bounds for the leptonic decays

$$\left(\frac{\text{Br}^{\text{exp.}}(\tau \rightarrow \nu_\tau e \bar{\nu}_e)}{\tau_\tau^{\text{exp.}}} \cdot \frac{1}{\Gamma_{\text{SM}}(\tau \rightarrow \nu_\tau e \bar{\nu}_e)} \right)^{1/2} = \cos \theta = 1.00201 \pm 0.00113 \quad (4.15)$$

$$\left(\frac{\text{Br}^{\text{exp.}}(\tau \rightarrow \nu_\tau \mu \bar{\nu}_\mu)}{\tau_\tau^{\text{exp.}}} \cdot \frac{1}{\Gamma_{\text{SM}}(\tau \rightarrow \nu_\tau \mu \bar{\nu}_\mu)} \right)^{1/2} = \cos \theta = 1.00204 \pm 0.00105 \quad (4.16)$$

Table 1. Table of branching ratios, decay constants, and CKM elements used.

$\text{Br}^{\text{exp.}}(\tau \rightarrow \nu_\tau e \bar{\nu}_e)$	0.1785 ± 0.0004	HFLAV [38]
$\text{Br}^{\text{exp.}}(\tau \rightarrow \nu_\tau \mu \bar{\nu}_\mu)$	0.17366 ± 0.00036	HFLAV [38]
$\text{Br}^{\text{exp.}}(\tau \rightarrow \pi \nu_\tau)$	0.1082 ± 0.0005	HFLAV [38]
$\text{Br}^{\text{exp.}}(\tau \rightarrow K \nu_\tau)$	$(0.697 \pm 0.010) \cdot 10^{-2}$	HFLAV [38]
f_{K^+}/f_{π^+}	1.1934 ± 0.0019	FLAG [34–36, 47–49]
f_{K^+}	$(155.7 \pm 0.3) \text{ MeV}$	FLAG [35, 36, 48–50]
f_{π^+}	$(130.5 \pm 0.3) \text{ MeV}$	
$ V_{ud} $	0.97367 ± 0.00032	PDG [37]
$ V_{us} $	0.22431 ± 0.00085	PDG [37]
$1/\alpha(m_\tau)$	133.50 ± 0.02	[51, 52]

and for the semi-hadronic decays

$$\left(\frac{\text{Br}^{\text{exp.}}(\tau \rightarrow \pi \nu_\tau)}{\tau_\tau^{\text{exp.}}} \cdot \frac{1}{\Gamma_{\text{SM}}(\tau \rightarrow \pi \nu_\tau)} \right)^{1/2} = \cos \theta = 0.99718 \pm 0.00453 \quad (4.17)$$

$$\left(\frac{\text{Br}^{\text{exp.}}(\tau \rightarrow K \nu_\tau)}{\tau_\tau^{\text{exp.}}} \cdot \frac{1}{\Gamma_{\text{SM}}(\tau \rightarrow K \nu_\tau)} \right)^{1/2} = \cos \theta = 0.99093 \pm 0.00880 \quad (4.18)$$

here we roughly estimated the errors by assuming they are all uncorrelated and distributed Gaussian. The leptonic decays all prefer unphysical values with $\cos \theta > 1$, the semi-hadronic decays, however, permit non-zero mixing angles. For the decay $\tau \rightarrow \pi \nu_\tau$ we find the mixing angle¹

$$\tau \rightarrow \pi \nu_\tau : \quad |\sin \theta| = (7.5 \pm 3.6) \cdot 10^{-2} \quad (4.19)$$

and for $\tau \rightarrow K \nu_\tau$ the mixing angle

$$\tau \rightarrow K \nu_\tau : \quad |\sin \theta| = (13.5 \pm 5.2) \cdot 10^{-2}. \quad (4.20)$$

In Fig. 13 we show the 1σ band of the cosines of the mixing angle as a function of the τ lifetime. Combining the semi-hadronic and leptonic decay yields $\cos \theta = 1.00181 \pm 0.00075$, combining only the two semi-leptonic decays leads to $\cos \theta = (9.96 \pm 0.04) \cdot 10^{-1}$ corresponding to

$$\tau \rightarrow P \nu_\tau \quad P = \pi, K \text{ combined} : \quad |\sin \theta| = (9.09 \pm 3.56) \cdot 10^{-2}. \quad (4.21)$$

¹For the central value and the error of the sine we have performed a Monte Carlo error propagation. The central value of the sine stems from the central value of the cosine e.g. $\arccos(0.99718) = 7.5014 \cdot 10^{-2}$. The error was estimated taking one standard deviation of $\sqrt{1 - \cos^2 \theta}$.

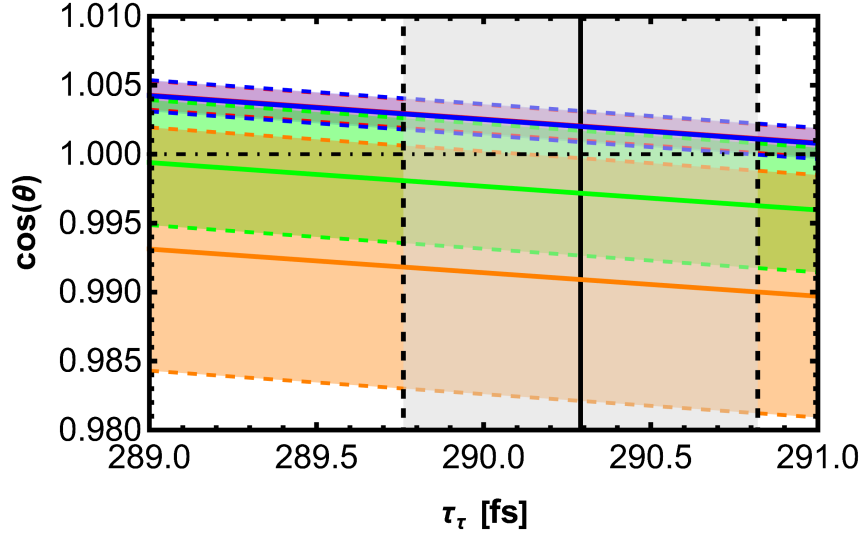


Figure 13. Cosine of the mixing angle vs. the τ lifetime. The grey band is the 1σ band of the world average of the τ lifetime. The solid lines are the central values and the dashed lines delimit the 1σ band. The bands from $\tau \rightarrow \nu_\tau e \bar{\nu}_e$ (blue) and $\tau \rightarrow \nu_\tau \mu \bar{\nu}_\mu$ (red) overlap. the constraints from both $\tau \rightarrow \pi \nu_\tau$ (green) and $\tau \rightarrow K \nu_\tau$ (orange) fully comply with the measured τ lifetime. The area under the dot-dashed line at $\cos \theta = 1$ delimits the physically allowed region.

4.5 Detecting HSN for $m_N < m_\tau$ from spectra

HSNs light enough to be produced in τ decays are difficult to detect in branching ratios, because

$$\Gamma(\tau \rightarrow \nu_\tau Y) + \Gamma(\tau \rightarrow N Y) = \Gamma_{\text{SM}}(\tau \rightarrow \nu_\tau Y) + \mathcal{O}\left(\frac{m_N^2}{m_\tau^2} \cdot \sin^2 \theta\right) \quad (4.22)$$

for $m_N < m_\tau$ and where Y is any final state. To this end one better employs precise measurements of the charged lepton energy spectrum

$$\frac{d\Gamma(\tau \rightarrow \nu \ell \bar{\nu}_\ell)}{dE_\ell} = \frac{G_F^2 m_\tau^4 V_\nu^2}{2\pi^3} F(x_E, x_\ell, x_\nu),$$

here $\nu = \nu_\tau, N$ is either a SM or a sterile neutrino, $x_E = E_\ell/m_\tau$, $x_i = m_i/m_\tau$, $V_\nu = \cos \theta$ for SM and $V_\nu = \sin \theta$ for sterile neutrinos, and

$$F(x_E, x_\ell, x_\nu) = \frac{\sqrt{x_E^2 - x_\ell^2} (1 - 2x_E + x_\ell^2 - x_\nu^2)^2}{6(1 - 2x_E + x_\ell^2)^3} \quad (4.23)$$

$$\times \left[8x_E^3 - 2x_E^2(5 + 5x_\ell^2 + x_\nu^2) \right. \\ \left. + x_E(3 + 10x_\ell^2 + 3x_\ell^4 + 3x_\nu^2(1 + x_\ell^2)) - 2x_\ell^2(1 + x_\ell^2 + 2x_\nu^2) \right].$$

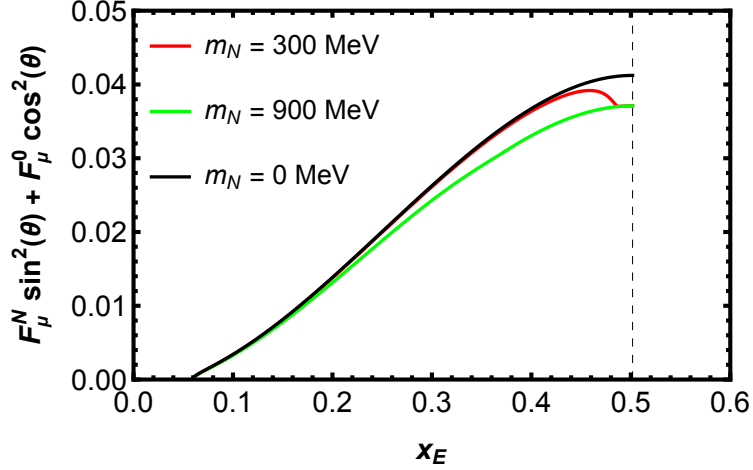


Figure 14. Here we show $F_\mu^N \sin^2 \theta + F_\mu^0 \cos^2 \theta = F(E_\mu/m_\tau, x_\mu, x_N) \sin^2 \theta + F(E_\mu/m_\tau, x_\mu, 0) \cos^2 \theta$ for $\ell = \mu$, the black line corresponds to the SM case $m_N = 0$, the mixing angle assumed here corresponds to $\sin \theta = 0.32$.

Since the experiment cannot distinguish between sterile and SM neutrino the measured lepton energy is

$$\begin{aligned} \frac{d\Gamma_{\text{lep}}^{\text{exp.}}}{dE_\ell} &= \frac{d\Gamma(\tau \rightarrow \nu_\tau \ell \bar{\nu}_\ell)}{dE_\ell} + \frac{d\Gamma(\tau \rightarrow N \ell \bar{\nu}_\ell)}{dE_\ell} \\ &= \frac{G_F^2 m_\tau^4 V_\nu^2}{2\pi^3} \left[F(x_E, x_\ell, x_N) \sin^2 \theta + F(x_E, x_\ell, 0) \cos^2 \theta \right]. \end{aligned} \quad (4.24)$$

The hadronic spectrum is derived analogously,

$$\frac{d\Gamma(\tau \rightarrow \nu X)}{ds} = N_c \frac{G_F^2 m_\tau^3 V_\nu^2 \cdot 2(|V_{ud}|^2 + |V_{us}|^2)}{192\pi^3} S(m_\tau, m_Z) G(x, x_\nu), \quad (4.25)$$

where $S(m_\tau, m_Z) = 1.01907$ [52, 53] accounts for electroweak corrections, $x = s/m_\tau^2$, $x_\nu = m_\nu/m_\tau$, and

$$\begin{aligned} G(x, x_\nu) &= \left[\left(1 + x_\nu^2 - x\right) \left(1 + 2x + x_\nu^2\right) - 4x_\nu^2 \right] \\ &\quad \times \sqrt{\lambda(1, x, x_\nu^2)} \cdot 12\pi \text{Im} \Pi_V^{1+0}(m_\tau^2 x). \end{aligned} \quad (4.26)$$

As for the leptonic decay the measured quantity is the sum of SM and sterile neutrino contributions

$$\begin{aligned} \frac{d\Gamma_{\text{had}}^{\text{exp.}}}{ds} &= \frac{d\Gamma(\tau \rightarrow \nu_\tau X)}{ds} + \frac{d\Gamma(\tau \rightarrow N X)}{ds} \\ &= N_c \frac{G_F^2 m_\tau^3 V_\nu^2 \cdot 2(|V_{ud}|^2 + |V_{us}|^2)}{192\pi^3} S(m_\tau, m_Z) \\ &\quad \times \left[G(x, x_N) \sin^2 \theta + G(x, 0) \cos^2 \theta \right]. \end{aligned} \quad (4.27)$$

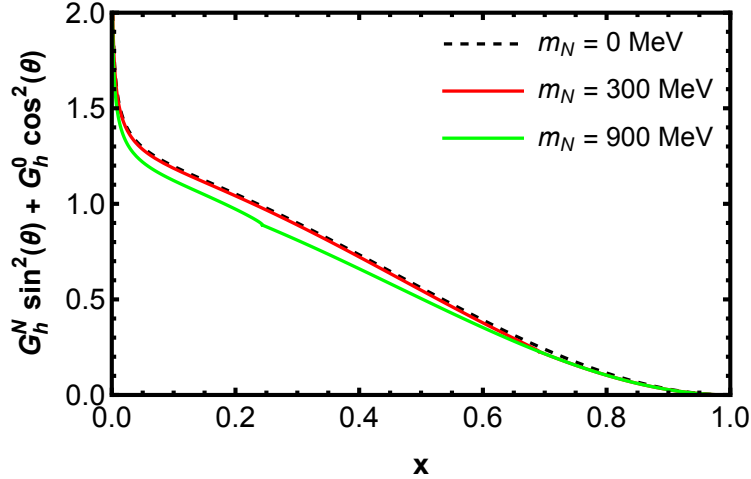


Figure 15. The plot shows $G_h^N \sin^2 \theta + G_h^0 \cos^2 \theta = G(s/m_\tau^2, x_N) \sin^2 \theta + G(s/m_\tau^2, 0) \cos^2 \theta$, the mixing angle is chosen to give $\sin \theta = 0.32$.

In Figs. 14 and 15 we show the spectrum for the leptonic decay with $\ell = \mu$ in the final state and the hadronic spectrum, respectively, in both cases with $\sin \theta = 0.32$. A HSN with a mass of $m_N = 300$ MeV leads to a significantly modified spectrum. The perturbative calculation of the hadronic spectrum can be compared to data for large $s \gtrsim 1$ GeV. In addition, one can compare integrated spectra from $s = 0$ to a chosen $s_{\text{max}} \gtrsim 1$ GeV, exploiting quark-hadron duality as described in Appendix B.

4.6 Comparisons

It is interesting to compare the allowed values of the mixing angle with other experimental exclusions. Both ATLAS [54] and CMS [55] have published upper and lower limits on the mixing angle. ATLAS did not perform the analysis for the HSN exclusively mixing with the τ neutrino. The CMS experiment specifically looked at ν_τ - N mixing and is insensitive to HSN masses with $m_N < 3$ GeV.

For $\mathbf{m}_N < \mathbf{m}_\tau$ we find from the τ lifetime for $m_N \approx 600$ MeV the allowed range $V_{N\tau} = \theta \lesssim 0.2$. This excludes mixing angles in a mass range not probed by CMS and ATLAS.

For $\mathbf{m}_N > \mathbf{m}_\tau$ we find the mixing angle in Eq. (4.10) from the τ lifetime. The semi-hadronic τ decays exclude mixing angles for HSN masses $m_N > m_\tau - m_P$ where $P = \pi, K$ and lead to Eq. (4.19) for $\tau \rightarrow \pi \nu_\tau$, and Eq. (4.20) for $\tau \rightarrow K \nu_\tau$. In combination, the semi-leptonic decays lead to Eq. (4.21), valid for $m_N > m_\tau - m_P$.

Thus we are able to exclude mixing angles for $m_N \in [m_\tau, 3 \text{ GeV}]$ not probed by the LHC. Recently it was pointed out that indeed the LHC might already be capable of probing mixing angles for mixing of sterile neutrinos with τ neutrinos [56]. A reinterpretation of the existing LHC data would be highly interesting.

4.7 BSM scenarios with other light invisible particles

Leptonic τ decays $\tau \rightarrow \nu_\tau \ell \bar{\nu}_\ell$ are interesting as there are two neutrinos produced in the final state: What is studied is $\tau \rightarrow \ell + E_{\text{miss}}$ and the squared missing mass is much larger than zero, so that there can be contributions from $\Gamma(\tau \rightarrow \ell X_{\text{dark}})$ or $\Gamma(\tau \rightarrow \ell X_{\text{dark}} X_{\text{dark}})$ with massive dark particles X_{dark} . A natural candidate for an invisible boson emitted in a τ decay is a majoron coupling to ν_τ [57–59].

We write Γ_{NP} for the dark contributions i.e. $\Gamma(\tau \rightarrow \ell + E_{\text{miss}}) = \Gamma(\tau \rightarrow \nu_\tau \ell \bar{\nu}_\ell) + \Gamma_{\text{NP}}$. This constrains the new physics contribution to

$$\Gamma_{\text{NP}} = \frac{\text{Br}^{\text{exp.}}(\tau \rightarrow \nu_\tau e \bar{\nu}_e)}{\text{Br}^{\text{exp.}}(\tau \rightarrow \pi \nu_\tau)} \Gamma_{\text{SM}}(\tau \rightarrow \pi \nu_\tau) - \Gamma_{\text{SM}}(\tau \rightarrow \nu_\tau e \bar{\nu}_e) = (3.94 \pm 3.81) \mu\text{eV} \quad (4.28)$$

$$\Gamma_{\text{NP}} = \frac{\text{Br}^{\text{exp.}}(\tau \rightarrow \nu_\tau \mu \bar{\nu}_\mu)}{\text{Br}^{\text{exp.}}(\tau \rightarrow \pi \nu_\tau)} \Gamma_{\text{SM}}(\tau \rightarrow \pi \nu_\tau) - \Gamma_{\text{SM}}(\tau \rightarrow \nu_\tau \mu \bar{\nu}_\mu) = (3.86 \pm 3.69) \mu\text{eV}, \quad (4.29)$$

where we set $\cos \theta = 1$ because of the tight constraints on $|\sin \theta|$ found above.

5 Conclusions

In this paper, we have calculated the inclusive semi-hadronic charged-current decay width of HSNs up to $\mathcal{O}(\alpha_s^4)$ in the strong coupling constant by using the known results of the electroweak gauge boson correlator which has been calculated up to the five-loop level. Decay rates into massless leptons can be trivially obtained from SM τ decay rates, while $N \rightarrow \tau + \text{hadrons}$ decays involve new phase-space integrals. We derive analytic expressions in terms polylogarithms (up to $\mathcal{O}(\alpha_s^3)$) and a series representation (valid for all calculated orders) for these rates. We then calculated the perturbative series and analyzed its stability in order to determine the sterile neutrino mass range for which the perturbative calculation is valid and robust theory predictions are possible. Reliable predictions for the semi-hadronic width are found for $m_N \geq 1.5 \text{ GeV}$ for $\ell = e, \mu$ in the final state. For the final state with $\ell = \tau$ we find stability for $m_N \geq 3 \text{ GeV}$. Our result can also be used for $\tau \rightarrow N + \text{hadrons}$ in the mass range $m_N \lesssim 600 \text{ MeV}$. In τ decays the perturbative series is only stable after including the $\mathcal{O}(\alpha_s^4)$ corrections.

We have further studied the impact of an N - ν_τ mixing angle θ on the τ lifetime. If N is light enough to be produced in τ decay, the SM decay amplitude is modified by a factor of $\cos \theta$ and there is an additional $\tau \rightarrow N + W^*$ mode with amplitude proportional to $\sin \theta$. We find the parameter space of m_N and θ constrained by the τ lifetime for HSN masses $m_N \lesssim 600 \text{ MeV}$, a region unconstrained by high- p_T data of the LHC. Furthermore, we present expressions for the lepton energy spectrum in

$\tau \rightarrow \ell \nu_\ell N$ and the hadron invariant mass spectrum in $\tau \rightarrow N + \text{hadrons}$, which may be used to detect HSN effects in the future.

HSNs heavier than the τ lepton may still leave imprints on observables through the cosine of the mixing angle. The lifetime analysis leads to $|\sin \theta| = (7.65 \pm 5.33) \cdot 10^{-2}$ in this case. For the four decays $\tau \rightarrow \nu_\tau \ell \bar{\nu}_\ell$ with $\ell = e, \mu$ and $\tau \rightarrow P \nu_\tau$ with $P = \pi^-, K^-$ we have compared the measured widths with the theoretical predictions. Only the data on the semi-hadronic decays permit a non-zero mixing angle and we derive the constraints $|\sin \theta| = (7.5 \pm 3.6) \cdot 10^{-2}$ from $\tau \rightarrow \pi \nu_\tau$ and $|\sin \theta| = (13.5 \pm 5.2) \cdot 10^{-2}$ from $\tau \rightarrow K \nu_\tau$, respectively. Combining both semi-hadronic decays leads to $|\sin \theta| = (9.09 \pm 3.56) \cdot 10^{-2}$. Our results are complementary to those from CMS, which constrain θ for HSN masses above 3 GeV. In another application of our calculation we have derived relative branching fractions between certain exclusive decays and the inclusive semi-hadronic decay and determined the fraction of $N \rightarrow \pi^+ \ell^-$ decays of all $N \rightarrow \ell^- + \text{hadrons}$ decays.

Finally we have derived a bound on the τ decay width into final states containing one or more new invisible particles, for example majorons. These decays contaminate $\tau \rightarrow \ell \bar{\nu}_\ell \nu_\tau$, whose decay rate is indeed a bit larger than the SM prediction. This finding calls for more precise experimental studies of the leptonic τ decays.

Acknowledgements

This research was supported by the Deutsche Forschungsgemeinschaft (DFG, German Research Foundation) under grant 396021762 - TRR 257 for the Collaborative Research Center *Particle Physics Phenomenology after the Higgs Discovery (P3H)*.

A QCD β -Function

We use the β -function with the following normalization

$$\frac{da_\mu}{d\ln\mu^2} = \beta(a_\mu) = -a_\mu^2 \left[\beta_0 + \beta_1 a_\mu + \beta_2 a_\mu^2 + \dots \right], \quad (\text{A.1})$$

where $a_\mu = a(\mu) = \alpha_s(\mu)/\pi$ and with the coefficients β_i [60, 61]:

$$\beta_0 = \frac{1}{4} \left(11 - \frac{2}{3} n_f \right), \quad (\text{A.2})$$

$$\beta_1 = \frac{1}{16} \left(102 - \frac{38}{3} n_f \right), \quad (\text{A.3})$$

$$\beta_2 = \frac{1}{64} \left(\frac{2857}{2} - \frac{5033}{18} n_f + \frac{325}{54} n_f^2 \right). \quad (\text{A.4})$$

Eq. (A.1) leads to

$$a(\mu) = a(\mu_0) - a(\mu_0)^2 \beta_0 \ell_{\mu\mu_0} + a(\mu_0)^3 \left[-\beta_1 \ell_{\mu\mu_0} + \beta_0^2 \ell_{\mu\mu_0}^2 \right] \quad (\text{A.5})$$

$$+ a(\mu_0)^4 \left[-\beta_2 \ell_{\mu\mu_0} + \frac{5}{2} \beta_0 \beta_1 \ell_{\mu\mu_0}^2 - \beta_0^3 \ell_{\mu\mu_0}^3 \right] + \mathcal{O}(a(\mu_0)^5), \quad (\text{A.6})$$

where $\ell_{\mu\mu_0} = \ln \left(\frac{\mu^2}{\mu_0^2} \right)$.

B Contour Integration

In the framework of perturbative calculations it is possible to calculate scattering or decay processes into quarks. However, in an experiment only hadrons are detectable and not quarks. This poses a problem as hadrons at different masses would appear as resonances in e.g. cross-sections. These resonances however are not accounted for by perturbative calculations using quarks. This conundrum was resolved by Poggio, Quinn and Weinberg [62]; they showed that a perturbative calculation smeared over a suitable energy range correctly averages over the resonances. This approach was then refined by showing that it is possible to transform the integration over the suitable energy range into an integration around a suitable complex contour [63, 64]. This was used for τ decays [20, 65], the integral in Eq. (3.2) can be rewritten in terms of a contour integration around a keyhole contour (see Fig. 16). Thus the decay width is proportional to the discontinuity over the branch cut along the positive real axis. In this way the integral may be rewritten in the following way (setting the lepton

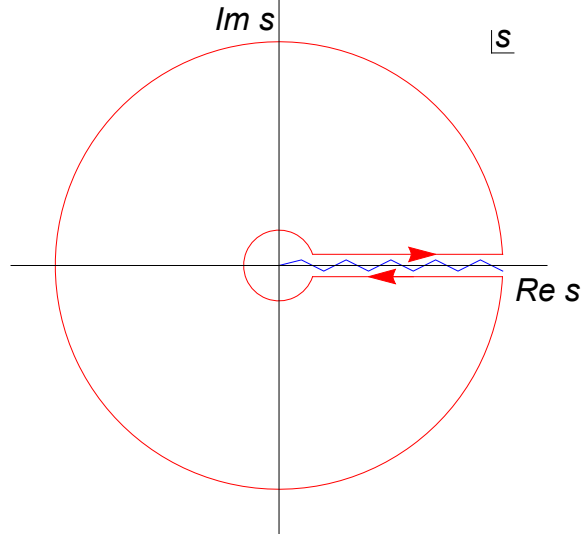


Figure 16. Contour integration permitting to replace the integral over the resonance region by the integral over the large circle, which is far away from resonances. Thus, while the differential spectrum is not perturbatively calculable in that region, the integrated spectrum is found correctly in this way.

mass to zero for brevity)

$$\begin{aligned} \Gamma(N \rightarrow X\ell) &\sim 12\pi \int_0^{m_N^2} ds \left(1 - \frac{s}{m_N^2}\right)^2 \left[\left(1 + 2\frac{s}{m_N^2}\right) \text{Im}\Pi^{(1+0)}(s) - 2\frac{s}{m_N^2} \text{Im}\Pi^{(0)}(s) \right] \\ &= 6\pi i \oint_{s=m_N^2} ds \left(1 - \frac{s}{m_N^2}\right)^2 \left[\left(1 + 2\frac{s}{m_N^2}\right) \Pi^{(1+0)}(s) - 2\frac{s}{m_N^2} \Pi^{(0)}(s) \right], \end{aligned}$$

the integral only depends on s at the value of the mass of the decaying particle and so low energy effects are already accounted for in the decay width. Indeed in this way the inclusive decay width correctly averages over all possible resonances induced by the mesons.

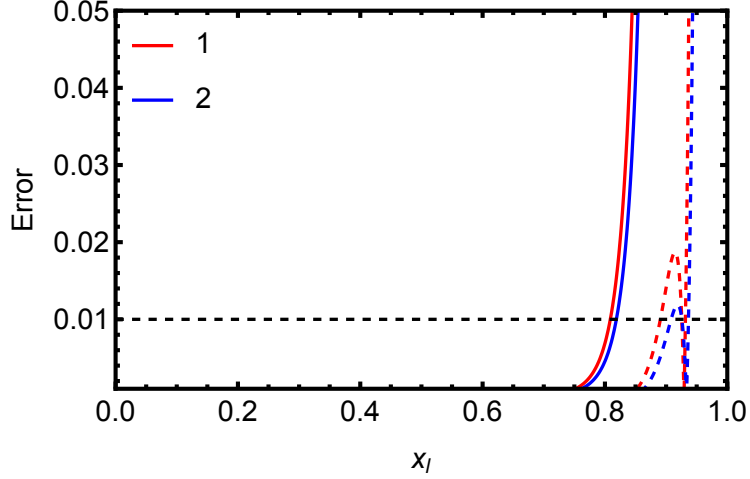


Figure 17. The absolute error $|1 - I_i^{\text{approx., T/P}}/I_i|$ of the approximations in Eqs. (C.1–C.4). The solid red and blue curves correspond to the Taylor expansion and the dashed blue and red curves are the polynomial fit. The dashed black line indicates the 1% level. For $x_\ell \lesssim 0.8$ both approximations have uncertainties $|1 - I_i^{\text{approx., T/P}}/I_i| < 1\%$.

C Easy-to-use Formulae for Phase-Space Integrals

For easier use we have expanded Eqs. (3.7), (3.8) as

$$I_1^{\text{approx., T}} = \frac{2}{525}x_\ell^{14} + \frac{1}{60}x_\ell^{12} + \frac{2}{15}x_\ell^{10} - \frac{43}{24}x_\ell^8 + \frac{34}{3}x_\ell^6 + \left(\frac{15}{2} - 2\pi^2\right)x_\ell^4 \quad (\text{C.1})$$

$$+ \frac{10}{3}x_\ell^2 - \frac{19}{24} + (x_\ell^4 - 8x_\ell^2 - 6)x_\ell^4 \log(x_\ell) + \mathcal{O}(x_\ell^{16})$$

$$I_2^{\text{approx., T}} = -\frac{787}{110250}x_\ell^{14} + \frac{1}{1800}x_\ell^{12} + \frac{217}{450}x_\ell^{10} + \frac{1}{6}(2\pi^2 - 5)x_\ell^8 \quad (\text{C.2})$$

$$+ \frac{2}{3}(37 - 4\pi^2)x_\ell^6 - 2(-12\zeta(3) + 3 + \pi^2)x_\ell^4 - \frac{56}{9}x_\ell^2 + \frac{265}{144}$$

$$- \frac{(8x_\ell^8 + 35x_\ell^6 + 280x_\ell^4 - 2100x_\ell^2 + 16800)x_\ell^6 \log(x_\ell)}{1050} + \mathcal{O}(x_\ell^{16}).$$

Additionally we have also fitted Eq. (3.7), (3.8) to polynomials

$$I_1^{\text{approx., P}} = 1.27683x_\ell^9 - 1.11042x_\ell^8 - 10.3142x_\ell^7 + 21.4421x_\ell^6 - 9.05503x_\ell^5 \quad (\text{C.3})$$

$$- 6.19752x_\ell^4 + 1.5042x_\ell^3 + 3.24256x_\ell^2 + 0.00309017x_\ell - 0.7917$$

$$I_2^{\text{approx., P}} = -4.83878x_\ell^9 + 29.1877x_\ell^8 - 53.4361x_\ell^7 + 34.6139x_\ell^6 - 7.13307x_\ell^5 \quad (\text{C.4})$$

$$+ 6.63816x_\ell^4 - 0.720101x_\ell^3 - 6.14877x_\ell^2 - 0.00323628x_\ell + 1.84032$$

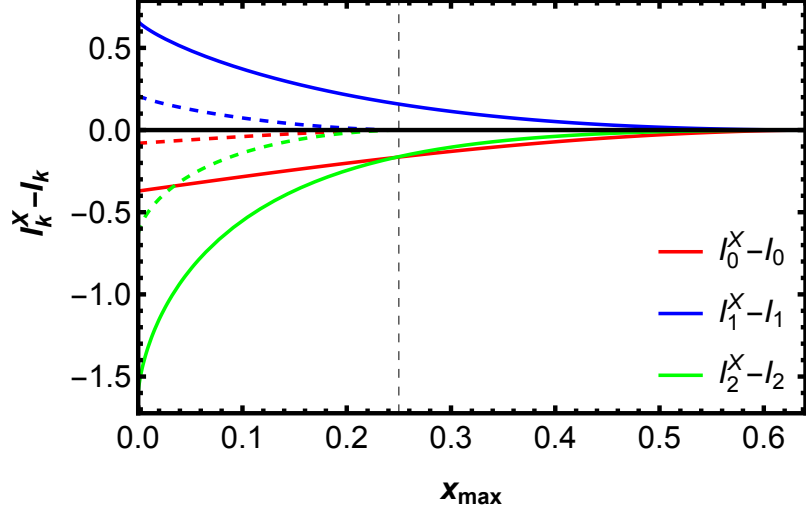


Figure 18. Here $I_k^X - I_k$ is plotted for two different values of $x_\ell = 0.2$ (closed line) and $x_\ell = 0.5$ (dashed line). The vertically dashed line lies at the end of the spectrum of the dashed curves i.e. $(1 - 0.5)^2 = 0.25$. At the end of the spectrum the $I_i^X - I_i = 0$

D Integrated Spectrum

Here we present the analytical solutions of the integral

$$I_k(x_\ell^2, x_{\max}) = \int_0^{x_{\max}} dx \left((1 + x_\ell^2 - x)(1 + 2x + x_\ell^2) - 4x_\ell^2 \right) \sqrt{\lambda(1, x, x_\ell^2)} \ln^k(x), \quad (\text{D.1})$$

for $k < 3$. In Fig. 18 the $I_k(x_\ell^2, x_{\max}) - I_k(x_\ell^2, (1 - x_\ell)^2)$ are shown.

The $I_k(x_\ell^2, x_{\max}) - I_k(x_\ell^2, (1 - x_\ell)^2)$, which we denote as $I_k^X - I_k$ and use $x_{\max} = \hat{x}$

as a shorthand notation, take the following form

$$I_0^X - I_0 = \frac{1}{2} \left(- \left(\hat{x}^2 + 7 \right) x_\ell^2 - (\hat{x} + 7) x_\ell^4 + x_\ell^6 \right. \quad (D.2)$$

$$\left. + (\hat{x} - 1)^2 (\hat{x} + 1) \right) \left(\hat{x} - (x_\ell + 1)^2 \right) X_r - 24 x_\ell^4 \text{ArcTanh}(X_r)$$

$$I_1^X - I_1 = 12 x_\ell^4 \left(\Delta \text{Li}_2 \left(- \frac{X_-}{2 x_\ell} \right) - \Delta \text{Li}_2 \left(\frac{X_-}{2} \right) + \Delta \text{Li}_2 \left(\frac{1 - X_r}{2} \right) \right) \quad (D.3)$$

$$+ \frac{1}{24} X_r \left(\hat{x} - (x_\ell + 1)^2 \right)$$

$$\times \left(- 3 \hat{x}^3 + 12 \left(- (\hat{x}^2 + 7) x_\ell^2 - (\hat{x} + 7) x_\ell^4 + x_\ell^6 + (\hat{x} - 1)^2 (\hat{x} + 1) \right) \ln(\hat{x}) \right.$$

$$\left. + 5(\hat{x}^2 + \hat{x}) + (\hat{x}(5\hat{x} + 4) + 85) x_\ell^2 + 5(\hat{x} + 17) x_\ell^4 - 19 x_\ell^6 - 19 \right)$$

$$+ \left(- 8 x_\ell^2 - 6 x_\ell^4 \left(4 \ln(\hat{x}) + 3 \ln \left(1 - X_r^2 \right) - 4 \ln(2) + 2 \right) \right.$$

$$\left. - 8 x_\ell^6 + x_\ell^8 + 1 \right) \text{ArcTanh}(X_r)$$

$$- \left(8 x_\ell^2 + 24 x_\ell^4 \ln(x_\ell) - 8 x_\ell^6 + x_\ell^8 - 1 \right) \text{ArcTanh} \left(- X_r \frac{1 + x_\ell}{1 - x_\ell} \right)$$

$$I_2^X - I_2 = X_r \left[\left((\hat{x}^2 + 7) x^3 - (\hat{x} - 1) (\hat{x}^2 + 3) x_\ell^2 + (\hat{x} + 3) x_\ell^6 + (\hat{x} + 7) x_\ell^5 \right. \quad (D.4)$$

$$\left. + (7 - 3\hat{x}) x_\ell^4 - (\hat{x} - 1)^2 (\hat{x} + 1) x_\ell + \frac{1}{2} (\hat{x} - 1)^3 (\hat{x} + 1) - \frac{x_\ell^8}{2} - x_\ell^7 \right) \ln^2(\hat{x})$$

$$+ \left(\frac{1}{12} (- 3 \hat{x}^4 + 8 \hat{x}^3 - 24 \hat{x} + 19) + \left(- 2 \hat{x} - \frac{11}{2} \right) x_\ell^6 - \frac{5}{6} (\hat{x} + 17) x_\ell^5 \right.$$

$$+ \frac{1}{6} (38 \hat{x} - 85) x_\ell^4 + \frac{1}{6} (- \hat{x} (5 \hat{x} + 4) - 85) x_\ell^3$$

$$+ \frac{1}{6} (\hat{x} (\hat{x} (4 \hat{x} - 3) + 38) - 33) x_\ell^2 + \frac{1}{6} (\hat{x} (\hat{x} (3 \hat{x} - 5) - 5) + 19) x_\ell$$

$$+ \frac{19 x_\ell^8}{12} + \frac{19 x_\ell^7}{6} \Big) \ln(\hat{x}) + \frac{1}{144} \left(9 \hat{x}^4 - 32 \hat{x}^3 + 288 \hat{x} - 265 \right)$$

$$+ \left(2 \hat{x} + \frac{113}{24} \right) x_\ell^6 + \frac{23}{72} (\hat{x} + 41) x_\ell^5 + \frac{1}{72} (943 - 446 \hat{x}) x_\ell^4$$

$$+ \frac{1}{72} (\hat{x} (23 \hat{x} + 28) + 943) x_\ell^3 + \frac{1}{72} (\hat{x} ((9 - 16 \hat{x}) \hat{x} - 446) + 339) x_\ell^2$$

$$+ \frac{1}{72} \left(\hat{x} ((23 - 9 \hat{x}) \hat{x} + 23) - 265 \right) x_\ell - \frac{265 x_\ell^8}{144} - \frac{265 x_\ell^7}{72} \Big]$$

$$+ x_\ell^4 \left[- 16 \mathcal{P}_{(0,7,5,0)} \text{ArcTanh}^2(X_r) \right]$$

$$\begin{aligned}
& + 24 \ln \left(1 - X_r^2 \right) \left(\text{Li}_2 \left(- \frac{X_- x_\ell}{X_+} \right) - \text{Li}_2 \left(- \frac{X_-}{X_+ x_\ell} \right) \right) \\
& + 24 \text{Li}_3 \left(- \frac{X_-}{X_+ x_\ell} \right) - 24 \text{Li}_3 \left(- \frac{X_- x_\ell}{X_+} \right) + 48 \text{Li}_3 \left(- \frac{X_-}{X_r - 1} \right) \\
& + 48 \text{Li}_3 \left(\frac{X_r + 1}{(X_r - 1) x_\ell} + 1 \right) + 24 \text{Li}_3 \left(- \frac{(X_r + 1) x_\ell}{X_r - 1} \right) \\
& + 24 \text{Li}_3 \left(\frac{x_\ell - X_r x_\ell}{X_r + 1} \right) + 30 \text{ArcTanh}(X_r) - 48 \zeta(3) \Big] \\
& + \frac{1}{6} x_\ell^8 \mathcal{P}_{(0,19,0,-3)} + x_\ell^6 \mathcal{P}_{(0,-\frac{46}{3},-2,4)} + x_\ell^2 \mathcal{P}_{(0,2,\frac{46}{3},-4)} \\
& + \ln(x) \left[x^8 \mathcal{P}_{(0,1,3,0)} - 8x^6 \mathcal{P}_{(0,1,3,0)} - 12x^4 \mathcal{P}_{(\pi^2,0,2,-1)} \right. \\
& + \ln(\hat{x}) \left(- 12x_\ell^4 \left(4 \text{ArcTanh}(X_r) + 1 \right) + 2x_\ell^8 - 16x_\ell^6 \right) \\
& - 12x_\ell^4 \ln^2(\hat{x}) + 48x_\ell^4 \ln(X_-) \text{ArcTanh}(X_r) \\
& + \ln(X_+) \left(- 24x_\ell^4 \left(2 \ln \left(1 - X_r^2 \right) + 2 \text{ArcTanh}(X_r) - 1 \right) - 4x_\ell^8 + 32x_\ell^6 \right) \\
& + 48x_\ell^4 \ln^2(X_+) + 96x_\ell^4 \text{ArcTanh}(X_r) \ln(1 - x_\ell) \\
& \left. - 16x_\ell^2 \text{ArcTanh}(X_r) + 2 \text{ArcTanh}(X_r) \right] \\
& + \ln^2(x_\ell) \left(12x_\ell^4 (2 \ln(X_+) - \mathcal{P}_{(0,2,0,0)}) + \frac{p(x_\ell)}{2} \right) - 12x_\ell^4 \ln^3(x_\ell) \\
& + \log(\hat{x}) \left[x_\ell^8 \mathcal{P}_{(\frac{19}{12},-2,0,0)} + x_\ell^6 \mathcal{P}_{(-\frac{26}{3},16,0,0)} + x_\ell^2 \mathcal{P}_{(\frac{26}{3},0,-16,0)} + \mathcal{P}_{(-\frac{19}{12},0,2,0)} \right. \\
& - 24x_\ell^4 \left(\text{Li}_2 \left(- \frac{X_-}{X_+ x_\ell} \right) - \text{Li}_2 \left(- \frac{X_- x_\ell}{X_+} \right) \right. \\
& \left. + 2 \text{ArcTanh}(X_r)^2 + \text{ArcTanh}(X_r) \right) - 2p(x_\ell) (\log(X_+) - \log(x_\ell + 1)) \Big] \\
& + \frac{1}{2} \log^2(\hat{x}) \left(p(x_\ell) - 48x_\ell^4 \text{ArcTanh}(X_r) \right) + 2 \ln^2(X_+) p(x_\ell) \\
& + \log(X_+) \left[\left(x_\ell^8 - 1 \right) \mathcal{P}_{(-\frac{19}{6},2,2,0)} - \left(x_\ell^4 - 1 \right) x_\ell^2 \mathcal{P}_{(-\frac{52}{3},16,16,0)} \right. \\
& + 48x_\ell^4 \left(\text{Li}_2 \left(- \frac{X_-}{X_+ x_\ell} \right) - \text{Li}_2 \left(- \frac{X_- x_\ell}{X_+} \right) \right) \\
& \left. - 4p(x_\ell) \log(x_\ell + 1) + 144x_\ell^4 \text{ArcTanh}^2(X_r) \right] \\
& + 48x_\ell^4 \text{ArcTanh}^2(X_r) \ln(X_-) \\
& + \log(1 - x_\ell) \left[8x_\ell^4 \left(6 \Delta \text{Li}_2 \left(\frac{X_-}{1 - X_r} \right) + 6 \Delta \text{Li}_2 \left(- \frac{X_-}{2x_\ell} \right) \right. \right.
\end{aligned}$$

$$\begin{aligned}
& -6\Delta\text{Li}_2\left(-\frac{1}{2}(X_r-1)(x_\ell+1)\right) \\
& -12\text{Li}_2\left(\frac{X_r+1}{2}\right) + 6\log(X_-)\left(\log(X_r+1) + \log\left(\frac{x_\ell+1}{2}\right)\right) \\
& -6\log(X_+)\left(\log\left(\frac{1-X_r}{2}\right) + \log(x_\ell+1)\right) + 6\log(2)\log\left(1-X_r^2\right) \\
& -6\log^2(X_r+1) + 12\text{ArcTanh}^2(X_r) + \pi^2 - 6\log^2(2) \\
& + 2p(x_\ell)\left(\log(\hat{x}) - 2\log(X_+) + \log\left(1-X_r^2\right)\right) \\
& + \frac{1}{6}\left(\mathcal{P}_{(0,0,-19,2)} + p(x_\ell)\left(6\text{Li}_2\left(-\frac{X_-}{X_+x_\ell}\right) + 6\text{Li}_2\left(-\frac{X_-x_\ell}{X_+}\right)\right.\right. \\
& \left.\left.+ 12\log\left(1-X_r^2\right)\log(x_\ell+1) + \pi^2\right)\right) \\
& + \text{Li}_2\left(\frac{X_-}{1-X_r}\right)q_+(x_\ell) - \text{Li}_2\left(\frac{X_+}{1+X_r}\right)q_-(x_\ell)
\end{aligned}$$

where the I_i are given in Eq. (3.6-3.8) and $X_r = \sqrt{(\hat{x} - (1-x_\ell)^2)/(\hat{x} - (1+x_\ell)^2)}$. We defined the following abbreviations

$$X_\pm = (1-x_\ell) \pm X_r(1+x_\ell), \quad (\text{D.5})$$

$$\mathcal{P}_{a,b,c,d} = a + b\ln(1-X_r) + c\ln(1+X_r) + d\ln^2(1-X_r^2) \quad (\text{D.6})$$

$$\Delta\text{Li}_n(f(X_r)) = \text{Li}_n(f(X_r)) - \text{Li}_n(f(-X_r)) \quad (\text{D.7})$$

$$p(x_\ell) = 1 - 8x_\ell^2 + 8x_\ell^6 - x_\ell^8 \quad (\text{D.8})$$

$$q_\pm(x_\ell) = 1 - 8x_\ell^2 - 12x_\ell^4 - 8x_\ell^6 + x_\ell^8 \quad (\text{D.9})$$

$$-24x_\ell^4\ln(\hat{x}) \pm 24x_\ell^4\ln\left(\frac{\hat{x}(1-X_r^2)}{X_+^2}\right)$$

where $f(X_r)$ is an arbitrary function depending on X_r .

Using Eq. (D.1) we plot the integrated decay width Γ_{cut} defined as

$$\begin{aligned}
\Gamma_{\text{cut}}(N \rightarrow \ell X) = & N_c \frac{G_F^2 m_N^5 |V_{N\ell}|^2}{192\pi^3} \\
& \times 2(|V_{ud}|^2 + |V_{us}|^2) \left[I_0 c_{0,1} + a_{m_N} c_{1,1} I_0 \right. \\
& + a_{m_N}^2 (c_{2,1} I_0 + 2c_{2,2} I_1) \\
& + a_{m_N}^3 (c_{3,1} I_0 + 2c_{3,2} I_1 - (\pi^2 I_0 - 3I_2) c_{3,3}) \\
& + a_{m_N}^4 (c_{4,1} I_0^Q + 2c_{4,2} I_1 \\
& \left. - (\pi^2 I_0 - 3I_2) c_{4,3} - (4\pi^2 I_1 - 4I_3) c_{4,4}) \right]
\end{aligned} \quad (\text{D.10})$$

where $I_k = I_k(x_\ell^2, x_{\text{max}})$.

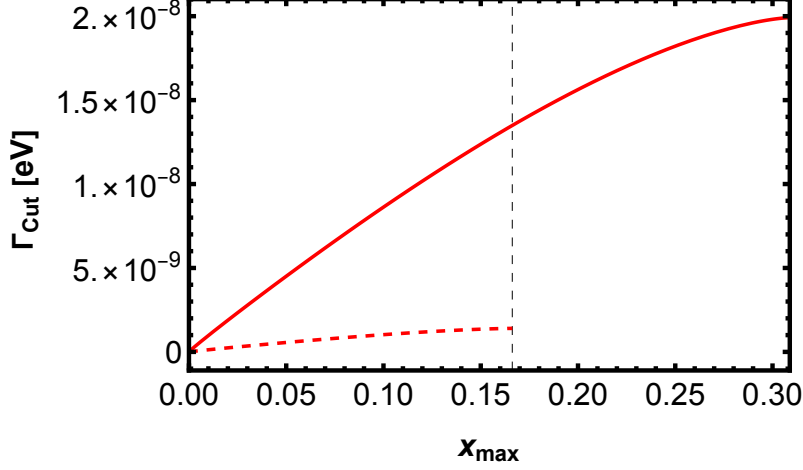


Figure 19. Integrated spectrum $\Gamma_N^X(x_{\max})$. The width is plotted with a mixing angle of $V_{N\ell} = 10^{-3}$ and the lepton is a tau $\ell = \tau$. In the full curve the mass of the HSN is $m_N = 4 \text{ GeV}$ whereas in the dashed curve it is $m_N = 3 \text{ GeV}$; the dashed vertical line marks the endpoint of the integrated spectrum for the dashed red curve.

References

- [1] T. Asaka and M. Shaposhnikov, *The ν MSM, dark matter and baryon asymmetry of the universe*, *Physics Letters B* **620** (2005) 17–26.
- [2] T. Asaka, S. Blanchet and M. Shaposhnikov, *The ν MSM, dark matter and neutrino masses*, *Physics Letters B* **631** (2005) 151–156.
- [3] M. Fukugita and T. Yanagida, *Baryogenesis Without Grand Unification*, *Phys. Lett. B* **174** (1986) 45.
- [4] S. Davidson and A. Ibarra, *A Lower bound on the right-handed neutrino mass from leptogenesis*, *Phys. Lett. B* **535** (2002) 25 [[hep-ph/0202239](#)].
- [5] T. Yanagida, *Horizontal gauge symmetry and masses of neutrinos*, *Conf. Proc. C* **7902131** (1979) 95.
- [6] P. Minkowski, *$\mu \rightarrow e\gamma$ at a Rate of One Out of 10^9 Muon Decays?*, *Phys. Lett. B* **67** (1977) 421.
- [7] K. Bondarenko, A. Boyarsky, D. Gorbunov and O. Ruchayskiy, *Phenomenology of GeV-scale heavy neutral leptons*, *Journal of High Energy Physics* **2018** (2018) .
- [8] D.J. Robinson, B. Shakya and J. Zupan, *Right-handed neutrinos and $R(D^{(*)})$* , *JHEP* **02** (2019) 119 [[1807.04753](#)].
- [9] F.U. Bernlochner, M. Fedele, T. Kretz, U. Nierste and M.T. Prim, *Model independent bounds on heavy sterile neutrinos from the angular distribution of $B \rightarrow D^* \ell \nu$ decays*, *JHEP* **01** (2025) 040 [[2410.11945](#)].
- [10] P.A. Baikov, K.G. Chetyrkin and J.H. Kuhn, *Order $\alpha^4(s)$ QCD Corrections to Z and τ Decays*, *Phys. Rev. Lett.* **101** (2008) 012002 [[0801.1821](#)].

- [11] M. Beneke and M. Jamin, α_s and the τ hadronic width: fixed-order, contour-improved and higher-order perturbation theory, *Journal of High Energy Physics* **2008** (2008) 044–044.
- [12] G. Cvetič and C.S. Kim, Rare decays of B mesons via on-shell sterile neutrinos, *Phys. Rev. D* **94** (2016) 053001.
- [13] L.M. Johnson, D.W. McKay and T. Bolton, Extending sensitivity for low-mass neutral heavy lepton searches, *Physical Review D* **56** (1997) 2970–2981.
- [14] V. Gribov, S. Kovalenko and I. Schmidt, Sterile neutrinos in tau lepton decays, *Nuclear Physics B* **607** (2001) 355–368.
- [15] D. Gorbunov and M. Shaposhnikov, How to find neutral leptons of the ν MSM?, *Journal of High Energy Physics* **2007** (2007) 015–015.
- [16] A. Atre, T. Han, S. Pascoli and B. Zhang, The search for heavy majorana neutrinos, *Journal of High Energy Physics* **2009** (2009) 030–030.
- [17] J.C. Helo, S. Kovalenko and I. Schmidt, Sterile neutrinos in lepton number and lepton flavor violating decays, *Nuclear Physics B* **853** (2011) 80–104.
- [18] J. Ellis, *TikZ-Feynman: Feynman diagrams with TikZ*, *Comput. Phys. Commun.* **210** (2017) 103 [1601.05437].
- [19] P.A. Baikov, K.G. Chetyrkin, J.H. Kühn and J. Rittinger, Complete $\mathcal{O}(\alpha_s^4)$ QCD Corrections to Hadronic Z Decays, *Phys. Rev. Lett.* **108** (2012) 222003.
- [20] E. Braaten, S. Narison and A. Pich, QCD analysis of the tau hadronic width, *Nuclear Physics B* **373** (1992) 581.
- [21] K. Chetyrkin, J. Kühn and A. Pivovarov, Determining the strange quark mass in cabibbo-suppressed tau lepton decays, *Nuclear Physics B* **533** (1998) 473–493.
- [22] C. Becchi, S. Narison, E. de Rafael and F.J. Yndurain, Light Quark Masses in Quantum Chromodynamics and Chiral Symmetry Breaking, *Z. Phys. C* **8** (1981) 335.
- [23] A. Pich, Precision physics with inclusive QCD processes, *Progress in Particle and Nuclear Physics* **117** (2021) 103846.
- [24] K.G. Chetyrkin, A.L. Kataev and F.V. Tkachov, Higher Order Corrections to $\sigma_{\text{tot}}(e^+e^- \rightarrow \text{Hadrons})$ in Quantum Chromodynamics, *Phys. Lett. B* **85** (1979) 277.
- [25] M. Dine and J. Sapiirstein, Higher-order quantum chromodynamic corrections in e^+e^- annihilation, *Phys. Rev. Lett.* **43** (1979) 668.
- [26] W. Celmaster and R.J. Gonsalves, Analytic calculation of higher-order quantum-chromodynamic corrections in e^+e^- annihilation, *Phys. Rev. Lett.* **44** (1980) 560.
- [27] S.G. Gorishnii, A.L. Kataev and S.A. Larin, Next-To-Leading $\mathcal{O}(\alpha_s^3)$ QCD Correction to $\sigma_{\text{tot}}(e^+e^- \rightarrow \text{Hadrons})$: Analytical Calculation and Estimation of the Parameter Lambda (MS), *Phys. Lett. B* **212** (1988) 238.

- [28] A.L. Kataev, *Next-next-to-leading perturbative QCD corrections: The Current status of investigations*, *Nucl. Phys. B Proc. Suppl.* **23** (1991) 72.
- [29] L.R. Surguladze and M.A. Samuel, *Total hadronic cross-section in e^+e^- annihilation at the four loop level of perturbative QCD*, *Phys. Rev. Lett.* **66** (1991) 560.
- [30] S.G. Gorishnii, A.L. Kataev and S.A. Larin, *The $O(\alpha_s^3)$ -corrections to $\sigma_{tot}(e^+e^- \rightarrow \text{hadrons})$ and $\Gamma(\tau^- \rightarrow \nu_\tau + \text{hadrons})$ in QCD*, *Phys. Lett. B* **259** (1991) 144.
- [31] S.L. Adler, *Some Simple Vacuum Polarization Phenomenology: $e^+e^- \rightarrow \text{Hadrons}$: The muonic-atom x-Ray Discrepancy and $g_\mu - 2$* , *Phys. Rev. D* **10** (1974) 3714.
- [32] K.G. Chetyrkin, J.H. Kuhn and M. Steinhauser, *RunDec: A Mathematica package for running and decoupling of the strong coupling and quark masses*, *Comput. Phys. Commun.* **133** (2000) 43 [[hep-ph/0004189](#)].
- [33] F. Herren and M. Steinhauser, *Version 3 of RunDec and CRunDec*, *Comput. Phys. Commun.* **224** (2018) 333 [[1703.03751](#)].
- [34] A. Bazavov et al., *B- and D-meson leptonic decay constants from four-flavor lattice QCD*, *Phys. Rev. D* **98** (2018) 074512 [[1712.09262](#)].
- [35] N. Carrasco et al., *Leptonic decay constants f_K, f_D , and f_{D_s} with $N_f = 2 + 1 + 1$ twisted-mass lattice QCD*, *Phys. Rev. D* **91** (2015) 054507 [[1411.7908](#)].
- [36] FLAVOUR LATTICE AVERAGING GROUP (FLAG) collaboration, *FLAG Review 2024*, [2411.04268](#).
- [37] PARTICLE DATA GROUP collaboration, *Review of particle physics*, *Phys. Rev. D* **110** (2024) 030001.
- [38] HEAVY FLAVOR AVERAGING GROUP (HFLAV) collaboration, *Averages of b-hadron, c-hadron, and τ -lepton properties as of 2023*, [2411.18639](#).
- [39] J. Erler and M. Luo, *Precision determination of heavy quark masses and the strong coupling constant*, *Phys. Lett. B* **558** (2003) 125 [[hep-ph/0207114](#)].
- [40] H. Lacker and A. Menzel, *Simultaneous Extraction of the Fermi constant and PMNS matrix elements in the presence of a fourth generation*, *JHEP* **07** (2010) 006 [[1003.4532](#)].
- [41] V. Cirigliano, D. Díaz-Calderón, A. Falkowski, M. González-Alonso and A. Rodríguez-Sánchez, *Semileptonic tau decays beyond the Standard Model*, *JHEP* **04** (2022) 152 [[2112.02087](#)].
- [42] T. Kinoshita and A. Sirlin, *Radiative corrections to Fermi interactions*, *Phys. Rev.* **113** (1959) 1652.
- [43] T. van Ritbergen and R.G. Stuart, *On the precise determination of the Fermi coupling constant from the muon lifetime*, *Nucl. Phys. B* **564** (2000) 343 [[hep-ph/9904240](#)].

- [44] M. Steinhauser and T. Seidensticker, *Second order corrections to the muon lifetime and the semileptonic B decay*, *Phys. Lett. B* **467** (1999) 271 [[hep-ph/9909436](#)].
- [45] Y. Nir, *The Mass Ratio m_c/m_b in Semileptonic b Decays*, *Phys. Lett. B* **221** (1989) 184.
- [46] A. Pak and A. Czarnecki, *Mass effects in muon and semileptonic $b \rightarrow c$ decays*, *Phys. Rev. Lett.* **100** (2008) 241807 [[0803.0960](#)].
- [47] N. Miller et al., *F_K/F_π from Möbius Domain-Wall fermions solved on gradient-flowed HISQ ensembles*, *Phys. Rev. D* **102** (2020) 034507 [[2005.04795](#)].
- [48] R.J. Dowdall, C.T.H. Davies, G.P. Lepage and C. McNeile, *V_{us} from π and K decay constants in full lattice QCD with physical u , d , s and c quarks*, *Phys. Rev. D* **88** (2013) 074504 [[1303.1670](#)].
- [49] EXTENDED TWISTED MASS collaboration, *Ratio of kaon and pion leptonic decay constants with $N_f = 2 + 1 + 1$ Wilson-clover twisted-mass fermions*, *Phys. Rev. D* **104** (2021) 074520 [[2104.06747](#)].
- [50] [FNAL/MILC 14A] A. Bazavov et al., *Charmed and light pseudoscalar meson decay constants from four-flavor lattice QCD with physical light quarks*, *Phys. Rev. D* **90** (2014) 074509 [[1407.3772](#)].
- [51] J. Erler, *Calculation of the QED coupling $\hat{\alpha}(M_Z)$ in the modified minimal subtraction scheme*, *Phys. Rev. D* **59** (1999) 054008 [[hep-ph/9803453](#)].
- [52] J. Erler, *Electroweak radiative corrections to semileptonic tau decays*, *Rev. Mex. Fis.* **50** (2004) 200 [[hep-ph/0211345](#)].
- [53] W.J. Marciano and A. Sirlin, *Electroweak radiative corrections to τ decay*, *Phys. Rev. Lett.* **61** (1988) 1815.
- [54] ATLAS collaboration, *Search for heavy neutral leptons in decays of W bosons using leptonic and semi-leptonic displaced vertices in $\sqrt{s} = 13$ TeV pp collisions with the ATLAS detector*, *JHEP* **07** (2025) 196 [[2503.16213](#)].
- [55] A. Hayrapetyan, A. Tumasyan, W. Adam, J.W. Andrejkovic, T. Bergauer, S. Chatterjee et al., *Search for long-lived heavy neutral leptons with lepton flavour conserving or violating decays to a jet and a charged lepton*, *Journal of High Energy Physics* **2024** (2024) .
- [56] E.D. Tireli, R.S. Klausen and O. Ruchayskiy, *Constraining Heavy Neutral Leptons Coupled to the Tau-Neutrino Flavor at the Large Hadron Collider*, [2510.12248](#).
- [57] Y. Chikashige, R.N. Mohapatra and R.D. Peccei, *Are There Real Goldstone Bosons Associated with Broken Lepton Number?*, *Phys. Lett. B* **98** (1981) 265.
- [58] G.B. Gelmini and M. Roncadelli, *Left-Handed Neutrino Mass Scale and Spontaneously Broken Lepton Number*, *Phys. Lett. B* **99** (1981) 411.
- [59] G. Barenboim and U. Nierste, *Modified majoron model for cosmological anomalies*, *Phys. Rev. D* **104** (2021) 023013 [[2005.13280](#)].

- [60] M. Czakon, *The four-loop qcd β -function and anomalous dimensions*, *Nuclear Physics B* **710** (2005) 485–498.
- [61] K. Chetyrkin, P. Baikov and J. Kühn, *The β -function of Quantum Chromodynamics and the effective Higgs-gluon-gluon coupling in five-loop order*, *PoS LL2016* (2016) 010.
- [62] E.C. Poggio, H.R. Quinn and S. Weinberg, *Smearing the Quark Model*, *Phys. Rev. D* **13** (1976) 1958.
- [63] R. Shankar, *Determination of the quark-gluon coupling constant*, *Phys. Rev. D* **15** (1977) 755.
- [64] C.S. Lam and T.M. Yan, *Decays of a heavy lepton and an intermediate weak boson in quantum chromodynamics*, *Phys. Rev. D* **16** (1977) 703.
- [65] E. Braaten, *QCD predictions for the decay of the τ lepton*, *Phys. Rev. Lett.* **60** (1988) 1606.